Uncertainties and their interaction in flood ~~risk~~hazard assessment with climate change

Hadush Meresa[1], Conor Murphy[1], Rowan Fealy[1], Saeed Golian[1]

[1]Irish Climate Analysis and Research UnitS (ICARUS), Dept. of Geography, Maynooth University, Maynooth, Ireland.
Correspondence to: Hadush Meresa (Hadush.Meresa@mu.ie)

Abstract

The assessment of future impacts of climate change is associated with a cascade of uncertainty linked to the modelling chain employed in assessing local scale changes. Understanding and quantifying this cascade is essential to developing effective adaptation actions. We evaluate and quantify uncertainties in future flood quantiles associated with climate change for four ~~Irish~~ catchments, incorporating within our modelling chain uncertainties associated with 12 Global Climate Models contained in the Coupled Model Intercomparison Project Phase 6, five different bias correction approaches, hydrological model parameter uncertainty and use of three different extreme value distributions for flood frequency analysis. Results indicate increased flood ~~risk~~hazard in all catchments for different Shared Socioeconomic Pathways (SSPs), with changes in flooding ~~related to~~ consistent with changes in annual maximum precipitation. We use ~~a sensitivity test based on the~~ additive chains and analysis of variance (ANOVA) to quantify and decompose uncertainties and their interactions in estimating selected flood quantiles ~~in the 2080s~~ for each catchment. We find that not only do the contributions of different sources of uncertainty vary by catchment, but that the dominant sources of uncertainty ~~vary between catchments, calling into question the ability to generalise about the importance of different components of the cascade~~can be very different on a catchment by catchment basis. While uncertainties in future projections are widely assumed to be dominated by the ensemble of ~~uncertainty~~climate models used, we find that ~~in future flood risk. For two~~one of our catchments~~,~~ uncertainties associated with bias correction methods ~~and~~dominate, while in another uncertainty associated with use of different extreme value distributions outweigh the uncertainty associated with the ensemble of climate models. ~~For all catchments and flood quantiles examined, hydrological model parameter~~These findings highlight the inability to generalise a priori about the importance of different components of the cascade of uncertainty ~~is the least important component of our modelling chain, while the uncertainties derived from~~in future flood hazard at the catchment scale. Moreover, we find that the interaction of components of the modelling chain employed are substantial (>20 percent of overall uncertainty in two catchments). While our sample is small, there is evidence that the dominant components of the cascade of uncertainty may be linked to catchment characteristics and rainfall–runoff processes. Future work that seeks to further explore the ~~dominant components~~ characteristics of the uncertainty cascade as

they relate to catchment characteristics may provide insight into a- priori identifying the key components of modelling chains to be ~~included~~targeted in climate change impact assessments.

Keywords: modelling, flood, climate change, uncertainty, impact, bias correction, GLUE, GR4J

1 Introduction

Climate change is likely to increasingly affect hydrological regimes and flood hazards over coming decades. ~~Significant~~Considerable changes in atmospheric temperature, precipitation, humidity, and circulation are expected, which may result in increasing extreme events, including floods (IPCC, 2013). ~~According to Rojas et al. (2013), flood frequency in Europe will increase due to climate change, with significant socio-economic implications for the region. Blöschl et al., (2017) and Blöschl et al., (2019) conclude that the timing and magnitude of European floods are shifting due to climate change and its consequences are not uniform across the region, with north western Europe experiencing earlier and higher flood peaks. Modelling and understanding of catchment scale flood risk~~. According to Rojas et al. (2013), flood frequency in Europe will increase due to climate change, with significant socio-economic implications for the region. Blöschl et al. (2017) and Blöschl et al. (2019) conclude that the timing and magnitude of European floods have shifted due to climate change and its consequences are not uniform across the region, with north-western Europe experiencing earlier and higher flood peaks. Modelling and understanding of catchment scale flood hazard projections is therefore an important endeavour for informing adaptation strategies.

~~However, this task~~Climate change impact assessment is subject to considerable uncertainties (Wilby and Dessai, 2010; Smith et al., 2018)~~.~~; Blöschl et al. (2019) recently highlighted uncertainty in hydrology as one of the 25 challenges in hydrological science. Traditional or top-down climate change impact assessments typically follow a modelling chain where output from Global Climate Models (GCMs), forced with estimates of future greenhouse gas concentrations, are extracted, and scaled to represent a study catchment. Hydrological models, calibrated for current conditions, are then forced with these GCM outputs to create discharge series spanning multiple decades into the future. When assessing flood ~~risk~~hazard, extreme value distributions are typically fitted to samples of extreme events (e.g. annual maximum flood series) representing current and future climates to evaluate changes in the characteristics of flooding. This modelling chain is replete with uncertainties that propagate and interact, resulting in potential large ranges ~~of~~in projected change at the catchment scale (e.g. Meresa, 2019) that can impede decision making (Smith et al., 2018). ~~Over recent decades many~~

Numerous studies have attempted to quantify the uncertainties in future climate change impacts due to the use of different climate models (e.g ~~Knutti & Sedláček, 2013)~~Knutti & Sedláček, 2013), natural variability (e.g. ~~Hughes et al., 2011)~~(Giuntoli et al., 2018; Hughes et al., 2011), bias correction techniques (e.g. ~~Kay et al., 2009; Saini et al., 2015; Soriano et al., 2019)~~ Kay

et al., 2009; Saini et al., 2015; Soriano et al., 2019), downscaling approaches (e.g. ~~Fowler et al., 2007;~~Fowler et al., 2007; ~~Gutmann et al., 2014),~~Gutmann et al., 2014), hydrological modelling uncertainties ~~(e.g. Wilby & Harris, 2006;~~ (e.g. Wilby &

65 Harris, 2006; Bastola et al., 2011; ~~Meresa & Romanowicz, 2017; Broderick et al., 2019)~~Addor et al., 2014; Meresa & Romanowicz, 2017; Broderick et al., 2019) and the application of different extreme value distributions for flood ~~risk~~hazard estimation (e.g. Meresa & Romanowicz, 2017; Lawrence, 2020). Findings from such studies confirm that the dominant source of uncertainty varies across studies. For example, Jobst et al. (2018)concluded that the GCM structure is the dominant contributor followed by emission scenario, bias correction, and hydrological model structure in New Zealand catchments.

70 Peleg et al. (2015) found that the hydrological regimes are highly sensitive to changes in convective precipitation in eastern Mediterranean catchments. Gosling et al. (2011) evaluated seasonal flow changes in UK catchments and found greater uncertainty in future estimates due to climate models than hydrological models. In Norwegian catchments Lawrence (2020) highlighted that climate models and frequency models are dominant sources of uncertainty in future flood projections. Therefore, the key components of the uncertainty cascade and their contributions tend to vary depend on the region,

75 precipitation type, and catchment.

Recognition of the uncertainties inherent in future climate ~~risk have~~change impacts has also given rise to novel approaches to decision-making that embrace uncertainties (e.g. Wilby & Murphy, 2019; Clark et al., 2016). Rather than aiming to derive precise assessments of future risk, such approaches aim to stress test and evaluate adaptation options, in static or dynamic ways

80 (Mazzorana et al., 2012), to identify actions that are functional across a range of plausible future conditions, rather than optimised to a certain outcome (e.g. structured decision making (SDM), robust decision making, decision scaling, adaptation pathways). ~~Each of these approaches require the cascade of uncertainty to be evaluated or navigated in ways that can better inform adaptation. For example, in Ireland~~Shepherd et al., (2018) recommend a storyline approach for navigating uncertainty, whereby examination of recent, notable extremes and the development of plausible narratives of change in their drivers enables

85 novel assessment of future changes, placing emphasis on physical processes. Each of these approaches require the cascade of uncertainty to be evaluated or navigated in ways that can better inform adaptation. For example, Broderick et al. (2019) employ a scenario neutral framework (Prudhomme et al., 2011) to evaluate design allowances for flood defences taking into account uncertainties derived from a large climate model ensemble, natural variability and hydrological models.

90 Whether employing traditional impact led or novel decision centric approaches, it is critical that key components of the cascade of uncertainty are adequately included. Research over the past two decades clearly shows that methodological choices made in assessing future climate change fundamentally impact on the portrayal of climate risk (Clark et al., 2016; Melsen et al., 2019). Top-down approaches must a-priori decide on the components of the modelling chain to include. Including all relevant components is typically a very resource expensive task (Smith et al., 2018) and it may not be apparent at the outset which

95 components of the modelling chain to include for specific catchments. For bottom up approaches, such as the scenario neutral method (Broderick et al., 2019), the modeller is forced to choose which aspects of uncertainty to prioritise in assessing

sensitivity to future changes. Again, this may not be apparent from the outset. It is widely acknowledged that climate models exhibit biases in their outputs (Krinner & Flanner, 2018; Giorgi & Gao, 2018), with numerous studies highlighting the need to post-process climate model output before use in simulating hydrological response (Ehret et al., 2012; Teng et al., 2012; Osuch et al., 2017; Meresa & Romanowicz, 2017). Dobler et al. (2012) suggest that the dominant components of the modelling chain may further vary depending on which part of the flow regime (low, mean, high flows) is of interest. They highlight, for example, that the importance of bias correction approaches to the overall uncertainty in hydrological response increases for high flows. Moreover, deep uncertainty can arise by virtue of the ad-hoc ways in which components of possible modelling chains are assembled and characterised within the overall modelling framework adopted (Wilby and Murphy 2019). Yet there are no established ways of sampling from the hierarchy of models used to evaluate impacts of climate change (Clark et al., 2016). Therefore, an important step in better integrating future climate risk into decision-making is the development of techniques that allow the contribution of different components of uncertainty and their interactions to be quantified and partitioned to help scientists and decision makers better navigate the cascade of uncertainty. In this regard ANOVA (ANalysis Of Variance) based techniques, which can be used to decompose sources of uncertainty and their interaction, offer significant utility (e.g. Kay et al., 2009; Vetter et al., 2016; Hattermann et al., 2018; Meresa, 2020).

In this study, we explore uncertainties in future flood risk for four Irish catchments and employ variance decomposition to quantify the contribution of various sources of uncertainty, together with their interaction, to the overall uncertainty in flood risk. In doing so we place emphasis on evaluating the uncertainties derived from; i) climate models in the newly available Coupled Model Inter-comparison Project Phase 6 (CMIP6) ensemble (Wyser et al., 2019); ii) widely used bias correction techniques; iii) hydrological model parameter uncertainty, and iv) the use of different extreme value distributions. The remainder of the paper is organised as follows; Section 2 outlines the study design and data/methods employed, Section 3 presents key results, exploring uncertainties for key steps in the modelling chain examined, together with their contributions and interactions to the full range of project change in flood risk. Section 4 provides a discussion of key insights, limitations and future directions before drawing main conclusions in Section 5.

2 Modelling and numerical experiments

Our study design is illustrated in Figure 1. We quantify uncertainties and their interaction in projected flood hazards using 12 Global Climate Models (GCMs) contained in the Coupled Model Inter-comparison Project Phase 6 (CMIP6) ensemble (https://esgf-node.llnl.gov/search/cmip6/), forced using three Shared Socioeconomic Pathways (SSP) scenarios. We use five bias correction techniques (Change factor (CF), Double Gamma Distribution Quantile (DGQM), Birnbaum distribution Quantile mapping (BQM), Single Gamma Distribution Quantile (SGQM), and Empirical Quantile (EQM)) to post-process climate model outputs (daily precipitation and air temperature time series). The daily bias corrected precipitation and temperature data are used as input to the Génie Rural à 4 paramètres Journalier (GR4J) hydrological model (Perrin et al., 2003).

GR4J has been previously applied to simulate high flows in Ireland, showing good performance in capturing a range of
hydrological signatures across diverse catchments (Broderick et al., 2019). The Generalized Likelihood Uncertainty Estimation
(GLUE) technique is used to quantify GR4J parameter uncertainty. In assessing future flood hazard the sensitivity of results
to different extreme value distributions is examined. In addition to evaluating each source of uncertainty independently, we
use variance decomposition to quantify the contribution of each methodological choice and their interactions to the overall
uncertainty in assessing flood risk. The climate change impact is evaluated based on relative future changes in the magnitude
of floods for the 2020s (2010-2039), 2050s (2040-2069) and 2080s (2070-2099) with respect to the reference period (1976-
2005). The following sections provide further details on the study catchments and each stage of the modelling chain employed.

2.1 Study catchments and hydro-climate datasets

Simulations are undertaken for four catchments (Boyne, Blackwater, Newport and Slaney), each representing different flood
response types across the Ireland as evaluated by Broderick et al. (2019). Their location, together with a summary of hydro-
climatic conditions for each catchment is summarized in Table 1 and Figure 2. Catchment area ranges from 146 km² (Newport)
to 2447 km² (Boyne), while elevation ranges from 56 m (Newport) to 112 m (Blackwater). For each catchment we use gridded
(1 × 1 km) daily precipitation and temperature data (Walsh, 2012) area averaged for the period 1976-2005 to provide a single
representative baseline series for each catchment. Daily potential evapotranspiration is derived using air temperature and
elevation following the method of Hamon (1964). This approach is favored over less parsimonious but more physically based
methods (e.g. Penman-Monteith), which have greater data input requirements (e.g. wind speed, humidity) not available for all
study catchments. Daily discharge data for each catchment was obtained from the Office of Public Works (OPW)
(**http://www.epa.ie/hydronet/**).

2.2 Climate Projections and Bias Correction

Daily precipitation (pr) and air temperature (tas) time series for the period 1971-2100 were extracted for 12 members of the
CMIP6 ensemble (https://esgf-node.llnl.gov/search/cmip6/) forced by each of three Shared Socioeconomic Pathway (SSP)
(SSP1, SSP3 and SSP5) scenarios (see Table 2 for details). For each catchment daily precipitation and air temperature were
extracted from the closest land-based GCM grid overlying the catchment centroid. It is widely acknowledged that climate
models exhibit biases in their outputs (Krinner & Flanner, 2018; Giorgi & Gao, 2018), with numerous studies highlighting the
need to post-process climate model output before use in simulating hydrological response (Ehret et al., 2012; Teng et al., 2012;
Osuch et al., 2015; Meresa & Romanowicz, 2017). However, there is still no consensus on which bias correction techniques
are most effective, nor in how bias correction techniques can modify future climate change signals. For instance, Teutschbein
& Seibert (2013) and Yang et al. (2010) showed distribution mapping based on theoretical distributions outperforms other bias
correction methods. Similarly, Berg et al. (2012) and Chen et al. (2013) and Berg et al. (2012) Chen et al. (2013) show that
theoretical distribution mapping performs similar to, or marginally better than, empirical quantile mapping. On the contrary,

160 Gudmundsson et al. (2012), Gutjahr & Heinemann, (2013) and Lafon et al. (2013), show that empirical quantile mapping demonstrates higher skill than theoretical distribution mapping in systematically correcting precipitation.

Moreover, deep uncertainty can arise by virtue of the ad-hoc ways in which components of possible modelling chains are assembled and characterised within the overall modelling framework adopted (Wilby and Murphy 2019). Yet there are

165 currently no established ways of sampling from the hierarchy of models used to evaluate impacts of climate change (Clark et al., 2016). Therefore, an important step in better integrating future climate risk into decision-making is quantifying and partitioning the contribution of different components of uncertainty and their interactions to help scientists and decision makers better navigate the cascade of uncertainty by identifying contributing sources that should be more fully explored (Smith et al., 2018). In this regard ANOVA (ANalysis Of Variance) based techniques, which can be used to decompose sources of

170 uncertainty and their interaction, offer considerable utility (e.g. Kay et al., 2009;Vetter et al., 2016; Hattermann et al., 2018; Meresa, 2020). In this study, we explore uncertainties in future flood hazard for four catchments, representative of different flood response types, in Ireland and employ additive chains and variance decomposition to quantify and examine the contribution of various sources of uncertainty, together with their interaction, to the overall uncertainty in flood hazard projections. In doing so we place emphasis on evaluating the uncertainties derived from; i) climate models in the newly

175 available Coupled Model Inter-comparison Project Phase 6 (CMIP6) ensemble (Wyser et al., 2019); ii) widely used bias correction techniques; iii) hydrological model parameter uncertainty, and iv) the use of different extreme value distributions. The remainder of the paper is organised as follows; Section 2 outlines the study design and data/methods employed, Section 3 presents key results, exploring uncertainties for key steps in the modelling chain examined, together with their contributions and interactions to the full range of projected change in flood risk. Section 4 provides a discussion of key insights, limitations

180 and future directions before drawing main conclusions in Section 5.

2 Models and Study Design

Our study design is illustrated in Figure 1. We quantify uncertainties and their interaction in projected flood hazards using 12 Global Climate Models (GCMs) contained in the Coupled Model Inter-comparison Project Phase 6 (CMIP6) ensemble (https://esgf-node.llnl.gov/search/cmip6/), forced using three Shared Socioeconomic Pathways (SSP) scenarios. We use five

185 bias correction techniques (Change factor (CF), Double Gamma Distribution Quantile (DGQM), Birnbaum distribution Quantile mapping (BQM), Single Gamma Distribution Quantile (SGQM), and Empirical Quantile (EQM)) to post-process climate model outputs (daily precipitation and air temperature time series). The daily bias corrected precipitation and temperature data are used as input to the Génie Rural à 4 paramètres Journalier (GR4J) hydrological model (Perrin et al., 2003). The Generalized Likelihood Uncertainty Estimation (GLUE) technique is used to quantify GR4J parameter uncertainty. In

190 assessing future flood hazard the sensitivity of results to different extreme value distributions is examined. In addition to evaluating each source of uncertainty independently, we use variance decomposition to quantify the contribution of each

methodological choice and their interactions to the overall uncertainty in assessing flood risk. The climate change impact is evaluated based on relative future changes in the magnitude of floods for the 2020s (2010-2039), 2050s (2040-2069) and 2080s (2070-2099) with respect to the reference period (1976-2005). The following sections provide further details on the study
195 catchments and each stage of the modelling chain employed.

2.1 Study catchments and hydro-climate datasets

Simulations are undertaken for four catchments (Boyne, Blackwater, Newport and Slaney), representing different flood response types across the Ireland (Broderick et al., 2019). Their location, together with a summary of hydro-climatic conditions for each catchment is summarized in Table 1 and Figure 2. Catchment area ranges from 146 km^2 (Newport) to 2447 km^2
200 (Boyne), while mean elevation ranges from 56 m (Newport) to 112 m (Blackwater). For each catchment we use gridded (1×1 km) daily precipitation and temperature data (Walsh, 2012) area averaged for the period 1976-2005 to provide a single representative baseline series for each catchment. Daily potential evapotranspiration is derived using air temperature and elevation following the method of Hamon (1964). This approach is favored over less parsimonious but more physically based methods (e.g. Penman-Monteith), which have greater data input requirements (e.g. wind speed, humidity) not available for all
205 study catchments. Daily discharge data for each catchment was obtained from the Office of Public Works (OPW) (**http://www.epa.ie/hydronet/**).

2.2 Climate Projections and Bias Correction

Daily precipitation (pr) and air temperature (tas) time series for the period 1971-2100 were extracted for 12 members of the CMIP6 ensemble (https://esgf-node.llnl.gov/search/cmip6/) forced by each of three Shared Socioeconomic Pathway (SSP) (
210 ~~Given these varied results, we~~SSP126, SSP370 and SSP585) scenarios (see Table 2 for details). For each catchment daily precipitation and air temperature were extracted from the closest land based GCM grid overlying the catchment centroid. We employ five commonly used techniques to bias correct raw climate model output and to examine the contribution of the selected bias correction methods to the total uncertainty in future flood hazard.

2.2.1 Change factor /delta change (CF)

215 The change factor technique applies multiplicative (for precipitation) and/or additive (for temperature) procedures for correcting raw model output. This involves correcting simulated daily precipitation ($P_{fut,corr}$) by multiplying the ratio of observed precipitation (P_{obs}) and reference precipitation simulation ($P_{ref,raw}$) to future simulations of raw climate model precipitation ($P_{fur,raw}$). For correcting future air temperature ($T_{fut,corr}$), the difference in observed air temperature (T_{obs}) and simulated temperature in the reference period ($T_{ref,raw}$) is added to raw climate output ($T_{fur,raw}$).

220

$$P_{fut,corr} = P_{fur,raw} * \frac{P_{obs}}{P_{ref,raw}}$$ (1)

$$T_{fut,corr} = T_{fur,raw} + (T_{obs} - T_{ref,raw})$$ (2)

2.2.2 Empirical quantile mapping (EQM)

225 Empirical quantile mapping is based on pair-wise comparison between the empirical cumulative density functions (ecdf) of observed and simulated daily precipitation time series during the reference period (1976-2005). This is a purely empirical andapproach with direct matching of the histogram of the observed precipitation to the future period. Future precipitation and temperature are corrected using the inverse of the ecdf ($ecdf^{-1}$) and fitted ecdf $ecdf_{hst,m}$.

230 $$P^{cor}_{hst,m} = (ecdf^{-1}_{obs,m}(ecdf_{hst,m}(P_{hst,m})))$$ (3)

$$T^{cor}_{hst,m} = (ecdf^{-1}_{obs,m}(ecdf_{hst,m}(T_{hst,m})))$$ (4)

The non-parametric quantile matching was performed first in the reference period (m, modeling period) using an exponential
235 transfer function assumption. Then the calibrated coefficients were used to correct the future daily precipitation and air temperature.

2.2.3 Distribution Quantile Mapping (DQM)

Distribution quantile mapping is a distribution parameter dependant bias correction technique. The parameters are extracted by fitting Gamma distribution to observed and simulated time series data, and matching its corresponding quantiles from the
240 observed and raw climate model output in the reference period (1976-2005) (Piani et al., 2010). We applied two types of DQM to correct climate biases: Single Gamma Distribution Quantile Mapping (SGDQM) and Double Gamma Distribution Quantile Mapping (DGDQM), together with the Birnbaum-Sanders distribution method (BSM) (Marzena Osuch et al., 2016). These methods also allow for theany excess in the number of dry, drizzle and wet days to be considered and corrected. In the case of SGQM, the first step is fitting a Gamma distribution to the upper 75 % of daily observed and raw climate output precipitation
245 distribution. Whereas in the DGDQM, the Gamma distribution is fitted to both the upper ≥ 75 % and to the lower < 75 % of the daily observed and raw climate output precipitation in the reference period (1976-2005). In both cases, non-rain days were removed and only wet days were considered. Similarly, BSM used the Birnbaum-Sanders distribution to transfer the precipitation quantile from the observed time series to raw output of the GCMs in the reference period.

250 $$P_{corr} = F^{-1}_{dg}(F_{dg}(P_{raw}(t), \alpha_{raw}, \beta_{raw}), \alpha_{Obs}, \beta_{Obs})$$ (5)

$$P_{corr} = F_{db}^{-1}(F_{db}(P_{raw}(t), \alpha_{raw}, \beta_{raw}), \alpha_{Obs}, \beta_{Obs}) \qquad (6)$$

$$T_{corr} = F_{db}^{-1}(F_{db}(T_{raw}(t), \alpha_{raw}, \beta_{raw}), \alpha_{Obs}, \beta_{Obs}) \qquad (7)$$

255

$$T_{corr} = F_{dn}^{-1}(F_{dn}(T_{raw}(t), \alpha_{raw}, \beta_{raw}), \alpha_{Obs}, \beta_{Obs}) \qquad (8)$$

Where P_{corr} and T_{corr} are the bias corrected daily precipitation and temperature, respectively. Likewise, $P_{raw}(t)$ and $T_{raw}(t)$ represent for raw climate model output for precipitation and temperature. The raw climate output inverse cumulative density

260 (CDF) is symbolized by F_{dg}^{-1}, F_{db}^{-1}, and F_{dn}^{-1} for precipitation and temperature, respectively. The dn, db and dg subscripts represent the normal (for temperature), Birnbaum-Sanders (for both precipitation and temperature) and Gamma (for precipitation) distributions, respectively. The Gamma (for precipitation) and Birnbaum-Sanders distributions have two parameters – the shape and scale parameters which are symbolised by α and β, and the normal (for temperature) distribution, with mean and standard deviation represented by μ and σ, respectively.

265 **2.3 Bias correction performance evaluation**

The performance of the selected bias correction techniques was evaluated using four statistical measures: Pearson Correlation (RR), Mean Absolute Error (MAE), Root Mean Square Error (RMSE) and Percent Bias (PBIAS). Evaluation was performed by comparing the ability of each approach to capture observed precipitation and temperature.

270

$$RR = \frac{\sum(P_S - \overline{P_S}) * (P_C - \overline{P_C})}{\sqrt{\sum(P_S - \overline{P_S})^2 * \sum(P_C - \overline{P_C})^2}} \qquad (9)$$

$$MAE = \frac{\sum_{i=1}^{n}|P_S - P_C|^{\wedge 2}}{N} \frac{\sum_{i=1}^{n}|P_S - P_C|}{N} \qquad (10)$$

$$PBIAS = \frac{\sum_{i=1}^{n}|P_S - P_C|}{\sum_{i=1}^{n} P_S} \qquad (11)$$

275

$$RMSE = \left[\frac{\sum_{i=1}^{n}|P_S - P_C|^2}{N}\right]^{0.5} \qquad (12)$$

Where Ps and Pc are observed and corrected precipitation, respectively, $\overline{P_C}$ is the mean of corrected precipitation, $\overline{P_S}$ the mean of observed precipitation and N is the number of observations.

2.4 Hydrological modelling

The GR4J model (Perrin et al., 2003) is a parsimonious four parameter, lumped conceptual rainfall-runoff model that has been widely applied in different hydro-climate conditions (Meresa & Gatachew, 2019; Meresa et al., 2017; He et al., 2018). The model is particularly suited to climate change impact studies given its parsimonious structure. GR4J simulates streamflow using precipitation, temperature and potential evapotranspiration (Perrin et al., 2003) and has previously been successfully used in Ireland to assess climate change impacts (Broderick et al. 2016; Broderick et al., 2019), river flow reconstructions (O'Connor et al., 2020) and seasonal hydrological forecasting (Donegan et al., 2020). Broderick et al. (2019) highlight the good performance of GR4J in capturing a range of hydrological signatures across diverse Irish catchments (Broderick et al., 2019). The model has two consecutive stores: one related to runoff production and the other to runoff routing. Detailed information about the model structure is given in ~~Perrin et al. (2003~~Perrin et al. (2003). The upper and lower limits of the four model parameters are listed in Supplementary Table S1. The model was calibrated and validated using observations over the period 1976-2005. The first four years were used as a model warmup to stabilise the initial states of the hydrological parameters. Calibration was undertaken from 1981-1999 and validation from 2000-2005. The Nash Sutcliffe Efficiency (NSE) objective function was used to evaluate the model performance and to identify behavioural parameter sets (Nash and Sutcliffe, 1970). NSE is defined as:

$$NSE = 1 - \frac{\sum_{t=1}^{j}(Q_{o,t}-Q_{m,t})^2}{\sum_{t=1}^{j}(Q_{o,t}-\bar{Q}_o)^2} \quad (13)$$

where $Q_{o,t}$ and $Q_{m,t}$ are observed and simulated flow at time t, Q_o is the mean observed flow and j is the length of the jth time series. The ability of hydrological model simulations to replicate the observations was further evaluated by deriving the proportion of extreme high flows inside the 95% confidence intervals (PCI). This is helpful for identifying a fixed NSE threshold for differentiating between behavioural and non-behavioural simulations (Li et al., 2011; Xu, 2014).

The Generalized Likelihood Uncertainty Estimation (GLUE) approach is widely applied to quantify hydrological model parameter uncertainty (Beven & Binley, 1992). GLUE is an informal statistical approach that uses Monte Carlo (MC) simulation to generate many possible hydrological parameter sets from specific ranges. The choice of the number of samples is somewhat subjective with studies typically employing a few thousand to tens of thousands of hydrological model parameter set samples to simulate river flow (Zheng and Bennett, 2002). In applying GLUE, we randomly generated ~~30,000~~a large number of parameter sets (30,000) using a uniform distribution~~) from~~ constrained by the acceptable ranges of each GR4J parameter. Behavioural parameter sets were identified based on ~~the~~ NSE (Equation 13) ~~weighting efficiency function and PCI (Equation (14), with a resultant fixed threshold of NSE ≥~~ scores >~~0.5 employed.~~50.

$$PCI = \left[1 - \left|\left(\frac{NQ_{t,p}}{T} - 0.95\right)\right|\right] * \frac{1}{T} * \left(\sum \frac{L_{u,t,p} - L_{t,t,p}}{Q_{o,t}}\right) \quad (14)$$

310 where $L_{L,t,p}$ and $L_{U,t,p}$ are the lower and upper boundary values of the extreme flow CI, T is the sum of time steps, $Q_{o,t}$ is the observed extreme flow at time step t, $NQ_{in,p}$ is the number of extreme peak flow observations which fall within the extreme flow CI. The shape of the 95% CI is governed by the value of PCI; if PCI is closer to 0.95 more of the observed time series extremes fall in the confidence interval band.

2.5 Flood frequency analysis

315 Numerous extreme value distributions can be deployed to estimate the frequencies of high flows. For example, the Log-Pearson III distribution is very popular in the USA and Australia for infrastructure design (Griffis & Stedinger, 2007), the General Extreme Value and Pearson Type III distributions are widely used in Europe (Madsen et al., 2013), while the Wakeby and Log-Normal distributions have been frequently used in Asia (Chen et al., 2012). However, a single distribution model may not be able to capture the entire temporal and spatial variability of hydrological extremes. Therefore, we employ three common

320 distribution types (LogN, Loglogistic LN, Log-logistic and GEV) with Maximum Likelihood parameter estimator (MLE) for flood frequency curve development. MLE estimates the distribution parameters by optimising the likelihood function of the cumulative probability distribution density, and its reliability is evaluated using the standard error of the estimated parameters. These distributions were fitted to the annual maximum daily peak flow flows in each study catchment. In Equations 15 – 17 14 - 16, the respective probability density function (PDF) of each distribution is presented. The GEV Log-Normal and Log-logistic

325 models have three two parameters, while the Log Normal GEV distribution has two three parameters.

Log-Normal (LN) $\qquad f(x) = \dfrac{\exp\left(-\frac{1}{2}\left(\frac{lnx-\mu}{\sigma}\right)^2\right)}{x\sigma\sqrt{2\pi}}$ $\qquad \sigma, \mu \ (\sigma>0)$ (14)

Log Logistic (LogL) $\qquad f(x) = \dfrac{\mu\left(\frac{x}{\sigma}\right)^{\mu-1}}{\sigma\left[1+\left(\frac{x}{\sigma}\right)^{\mu}\right]^2}$ (15)

GEV $\qquad f(x) =$

330 $\begin{cases} \frac{1}{\sigma}\exp\left(-(1+k(\frac{x-\mu}{\sigma}))^{\wedge-\frac{1}{k}}\right)\left(1+k(\frac{x-\mu}{\sigma})\right)^{-1-\frac{1}{k}} & k \neq 0 \\ \frac{1}{\sigma}\exp\left(-(\frac{x-\mu}{\sigma})-exp(-((x-\mu)/\sigma))\right) & k = o \end{cases}$ $\qquad$ K, σ, $\mu \ (\sigma>0)$

(16)

Where, σ is the scale, μ is location and k is the shape parameter.

2.6 Uncertainty ~~estimation and~~ decomposition ~~and estimation~~

We used two approaches to uncertainty analysis in future flood hazard. First is the additive chain approach which is similar to sensitivity analysis. whereby the main goal is to assess components of the modelling chain independently. Second, we used ANOVA to separate the variance contribution of each component of the modelling chain and their interaction. Unlike the former (sensitivity approach), it helps us to understand the interaction of factors and their main variables.

2.6.1 Additive chain approach

We examine the relative contribution of four key components of the modelling chain to the projected uncertainty in future flood ~~risk~~hazard. These are climate models (CM), bias correction techniques (BC), hydrological model parameters (HP) and flood frequency distribution models (FF). ~~For uncertainty decomposition, we~~ We only use a single SSP scenario (here ~~SSP3),~~SSP370) in our evaluation of the uncertainty cascade, with the assumption that different studies will be interested in quantifying flood ~~risk~~hazard for different emissions outcomes separately. ~~Unlike~~

Overall uncertainty is estimated based on the additive ~~or multiplicative~~chain method, while decomposition of the contribution of different sources of uncertainty and their interactions is evaluated using ANOVA. The uncertainty in future flood hazard can be defined as the total uncertainty resulting from the components (s) of the modelling chain considered – here four components $s1$ to $s4$ (CM, BC, HP and FF). Initially we define the cumulative uncertainty for each component (s) of the modelling chain denoted by $U^{cum}(X_1 \ldots X_s)$ and conditional probability as $U(q_{x\ s+1 \ldots xs})$. The uncertainty in our modelling chain is characterized as the total variance in the flood quantile generated from each of the four components evaluated, with total uncertainty defined as;

$$U^{cum}(x_1, \ldots, x_s) = \frac{1}{\pi_{j=s+1}^{nj}} \sum_{x_{s+1} \epsilon x_{s+1}} \cdots \sum_{x_s \epsilon x_s} U(q_{x\ s+1 \ldots xs}) \underline{\hspace{3cm}} (17)$$

This uncertainty quantification method keeps summing as the number of components (s) of the modelling chain increases. Therefore, the uncertainty of a particular step along the modelling chain e.g. s=4, denoted by $U^{cum}(X_s)$, can be described as:

$$U^{cum}(X_s) = U^{cum}(X_1, \ldots, X_s) - U^{cum}(X_1, \ldots, X_{s-1}) \underline{\hspace{3cm}} (18)$$

Note that uncertainty of each component of the chain is a magnitude of contribution to the total uncertainty so that the sum of uncertainties of individual sources is always equal to the cumulated uncertainty $U^{cum}(X_1, \ldots, X_s)$.

2.6.2 ANOVA approach

Unlike single chain based additive approaches to uncertainty estimation, ANOVA can decompose the aggregated source of
uncertainty into individual components and their interaction using specific extreme flow indices (Meresa & Romanowicz,
2017). We develop a hypothesis test using an ANOVA model that can identify the effect of each component (CM, BC, HP,
FF) in the model chain to the total variance of the extreme index (Y). According to n-way ANOVA principles, the model splits
the total sum of squares (SST) into the sum of squares (SS) of the main variables and their interactions as follows:

$$SST = \sum_{i=1}^{NCM=12} \sum_{j=1}^{NBC=5} \sum_{k=1}^{NHP=300} \sum_{l=1}^{NFF=3} (Y_{ijkl} - \bar{Y})^2 \qquad (\text{18}19)$$

Where Y_{ijkl} is estimated flood magnitude considering i=12 climate models, j=5 bias correction methods, k=300 hydrological
parameter sets, l=3 extreme frequency distributions, and $\bar{Y}$ is the mean of all variables. SST is athe grand square deviation of
the main and interacting variables. Further, the deviation in SST is split into the individual and interacting components to
explore their effect on the aggregated extreme flood frequency indices as follows:

$$SST = SS_{CM} + SS_{BC} + SS_{HP} + SS_{FF} + SS_{CMBC} + SS_{CMHP} + SS_{CMFF} + SS_{BCHP} + SS_{BCFF} + SS_{HPFF} \qquad (\text{19}20)$$

where SS_{CM} is the sum of standard errors of climate models, SS_{BC} is the sum of standard errors of bias correction methods,
SS_{HP} the sum of standard errors of hydrological parameters and SS_{FF} is the sum of the standard errors of flood frequency. In
examining combined effects, SS_{CMBC} is the sum of standard errors of climate models and bias correction methods, SS_{CMFF} the
sum of standard errors of climate models and extreme frequency, and SS_{BCHP} is the sum of standard errors of bias correction
methods and hydrological parameters.

3. Results

3.1 Evaluation of bias correction techniques

The annual maximum daily precipitation series from 12 GCMs were evaluated against observations for each catchment during
the period 1976-2005 (reference period). RR, MAE, PBIAS and RMSE results for each catchment are presented in Figure 3
and Figure S1. Following bias correction, results indicate an improvement of the GCMs in reproducing observed annual
maximum precipitation. However, the performance of each bias correction method is not uniform for all catchments and
GCMs. MAE values range from 0 to 195, RMSE 0 to 40, PBIAS -65 to 40, and RRR ranges from -0.40 to 0.50. Overall, the
distribution based bias correction methods performed better in reproducing observed maximum precipitation in these
catchments. The smallest PBIAS is observed in the Boyne catchment and largest in the Newport catchment. The BC-CCSM
and ACCES CM2 climate models show high RR (0.4) in the Slaney catchment using DGQM, SGQM and BSM. Whereas
GFDL and MPIESM-LR climate models indicates lower performance in correcting precipitation using all bias correction
methods. Figure 4 shows the raw GCM outputs together with the results of the five bias correction methods applied to the
CMIP6 ensemble in simulating monthlythe maximum daily precipitation in each month for each catchment. The corrected
monthly precipitation gives a wider spread in winter months (except DGQM and EQM techniques), relative to summer months.

However, the ensemble spread is dependent on the bias correction method. DGQM and EQM methods result in a relatively
395   narrower spread ~~in monthly simulations~~, whereas SGQM, BSM and CF return a wide range of simulations (Figure 4).

The influence of each bias correction method on the magnitude of simulated changes in annual maximum daily precipitation
for the 2050s (2040-2069) and 2080s (2070-2099) (relative to reference period: 1976-2005) was evaluated for each GCM SSP
combination (Figure 5). Simulated changes from the same 12 GCMs using different bias correction approaches show
400   substantial differences in the magnitude of changes in annual maximum precipitation. Generally, projected changes are smaller
in the Slaney and Boyne using DG methods, whereas the changes in the Blackwater and Newport are smaller using EQ and
SG. There is also a linear relationship between the annual maximum precipitation changes suggested for the 2050s and 2080s,
for most bias correction techniques and catchments, indicating a positive trend in the magnitude of changes with time (Figure
5). However, we note that there is greater scatter for EQM relative to other bias correction techniques and in the Blackwater
405   catchment relative to other catchments. We also note that the magnitude of change in annual maximum daily precipitation
tends to be higher for ~~SSP5~~SSP585 than for ~~SSP3~~SSP370 and ~~SSP1~~SSP126 and slightly higher in the Slaney and Newport
catchments, relative to the Boyne and Blackwater. Changes in annual maximum daily precipitation for SSP126 are smaller
than those simulated for SSP370 and SSP585 due to the lower radiative forcing and socio-economic impact associated with
SSP126 relative to other scenarios.
410

~~A similar evaluation was undertaken for mean annual air temperature for each catchment. Figure 6 shows the bias corrected~~
~~projected mean annual temperature for each catchment under each GCM/SSP combination, together with the ensemble median~~
~~for each SSP. The selected catchments show continuous warming during the 21st century. The ensemble mean changes for~~
~~SSP1, SSP3, and SSP5 scenarios are projected to be 10-12°C, 11-13.3°C, and 12-15°C, respectively by the end of the century.~~
415   ~~The spread at the end of 21st century is somewhat wider than the earlier periods. Bias correction results for precipitation are~~
~~shown in Figure S2 and for temperature in Figure S3.~~

3.2 Hydrological modelling and parameter uncertainty evaluation

~~Using the GR4J hydrological model, 30,000~~The GLUE procedure was used to identify a set of model parameters that offer
420   acceptable performance. Thirty thousand parameter sets were randomly generated from uniform distributions with the NSE
objective function threshold ~~set to~~of > 0.5, calculated from daily mean flows used to identify behavioural parameter sets.
~~Figure 7 shows the seasonal maximum flow~~To produce future simulations ~~derived~~, we employ the top 300 behavioural
parameter sets. Figure S3 shows the variation in model parameter values and NSE for each GR4J model parameter and
catchment. The majority of parameters show clearly identified peaks for each catchment, particularly the parameters X2, X3
425   and X4. The only parameter to show a lack of identifiability is the X1 parameter (the production storage capacity) in the
Newport catchment. This is the smallest of the four catchments and displays large variability in topography, landcover

(forestry) and has a lake present in the catchment. Figure 6 shows the ability of the GR4J model to simulate the maximum daily flows in each month using behavioural sets relative to observations for the years 1976-2005, together with the 9095 percent confidence intervals of the simulations. Monthly maximum simulationsSimulations successfully capture the observations, which mostly fall within the 95% and 5% percent confidence interval, except in the Boyne catchment, where a portion of the observed maximum flow time series fall outside of the simulated confidence interval. We note that the Boyne catchment has undergone significant arterial drainage works, which is likely to result in higher peak flows (Harrigan et al., 2014) in the observations relative to the model simulated values. GR4J achieved the best fit in the 95% CI modelling discharge in the Newport catchment. Overall, the model was able to capture winter flows well in all catchments, particularly winter peak flow simulations. The biggest discrepancies were observed in modelled flows during late summer, with poorer performance likely associated with use of the NSE objective function which is more sensitive to the large peak values than lower flows in summer.

Ensemble median projections of monthly maximum flow derived from 12 GCMs under SSP3 and 5 bias correction techniques for each catchment for the period 1976 to 2100 are shown in Figure 8. Increases are largest during the winter and early spring months in the Blackwater and Newport catchments, with maximum flow increasing from 17 m³/s to 25 m³/s during winter in the Newport catchment, and from 120 m³/s to 160 m³/s in the Blackwater. Also, the projected flows during late autumn and early summer periods shows the same trend and uniform pattern, with a maximum flow rate of about 35 m³/s for the Blackwater, 5 m³/s for Newport, 40 m³/s for the Boyne and 15 m³/s for the Slaney.

We examined the uncertainty associated with model parameters for different GCMs and future time periods. Figure 7 shows the simulated annual maximum daily flow for the reference and each future time period using the 300 GR4J behavioural parameter sets forced with 12 GCMs bias corrected using DGQM. It is evident that the uncertainty associated with hydrological model parameters is not static and varies depending on climate model, catchment and future time period. The importance of hydrological model uncertainty tends to be greatest for climate models that project the largest magnitude of change indicating that the changing characteristics of precipitation (e.g. mean and variability) have a large bearing on the importance of hydrological model uncertainty. It is also likely that different bias correction techniques interact with parameter uncertainty. The uncertainties associated with hydrological model parameters tend to be greatest for the 2080s (black lines in Figure 7), and for the Boyne and Slaney catchments.

Percent changes in maximum annual daily flow simulated using each of thebehavioural parameter sets, 12 GCMs bias corrected by each of the five methods, together with the raw simulations are presented in Figure 98. A clear increase in the annual maximum flow is suggested using DGQM, SGQM, CF, EQM and BSM, however, the magnitude of simulated increases differs depending on bias correction approach and are not uniform across the selected catchments. Overall, distribution based bias correction models give smaller changes in annual maximum flow time series. This indicates that wet-day frequency correction

is very important for understanding future annual maximum flow projections. Annual maximum flow changes using EQM gives a higher spread range and uncertainty~~.~~ in each catchment, while the change factor method produces the most modest changes. Changes in annual maximum flow are smallest in the ~~Boyne catchment and largest in the Newport~~Blackwater, which is notable as the catchment~~.~~ with largest groundwater storage. Changes in annual maximum flow are more constrained under ~~SSP3 and SSP5,~~SSP126 than ~~SSP1~~SSP370 and SSP585, however differences between SSPs are modest and uncertainty ranges of changes in annual maximum flow are considerable for each (Figure ~~9~~8).

3.3 Flood ~~hazard~~quantile projections under varying climate conditions

~~To evaluate changes in flood frequency we use the Akaike Information Criteria (AIC) to identify the best fitting distribution type in the reference period and observed time series for each GCM projection and catchment. Figure 10~~Figure 9 shows the estimated flood quantile values at different return periods (from 2 year to 100 year) using GEV, ~~LogN~~LN and LogL distribution models, and associated 95% confidence intervals from 12 GCMs (under ~~SSP3~~SSP370 scenario) bias corrected using the DGQM method over the full simulation period (1976-2100). Overall, the ~~LogL~~LogN distribution returned the smallest ~~changes~~ in flood ~~quantiles~~quantile magnitude and the narrowest uncertainty band, while the estimated quantile values using LogL tend to be the largest across each catchment. The GEV distribution gives the largest uncertainty ranges in flood quantiles in all catchments (Figure ~~10~~9).

~~Flood quantile changes~~Percent changes in flood quantiles for return periods ranging from 10 to 50 years were also evaluated for each future period under ~~SSP3~~SSP370 using ~~the~~ensemble mean of three distribution types fitted to the median GR4J simulation combining all GCMs and bias correction methods (Figure 10); and Figure flood Figure S4 shows quantile using GEV distribution fitted to the median GR4J simulation combining all GCMs and DGQM bias correction ~~methods~~method (Figure ~~11 and Figure~~ S4). Each catchment shows a significant increase in the magnitude of flood ~~quantile magnitudes~~quantiles in the future. Overall, changes in flood quantiles are consistent with changes in annual maxima daily flow. However, future flood ~~quantile~~ changes are not the same across catchments and differences exist based on bias correction methods employed. ~~The frequency of the larger return period flood (100-year flood) increases to higher than once in 20 years. The smallest changes (0-15%) in flood quantiles are observed in the Slaney using DGQM, the Boyne using SGQM and DGQM, Newport using CF and EQM, and in the Blackwater using CF. For the 100-year flood, the~~ The largest changes in ~~magnitude (50-200%) are noted using EQM in the selected catchments. By comparison, the other bias correction methods are consistent and indicate changes of between 30-50% in the Slaney and Boyne, and 50-100% in Blackwater and Newport in the future. Overall, the Slaney catchment shows smaller relative change in flood quantiles (0-20%) at different return periods using BSM, SGQM and CF, similarly using the DGQM projected changes range from 0-15%. Moreover, changes in extreme~~ flood quantiles ~~do not increase linearly from the~~ across all catchments are found using the BSM bias correction method, where in the Blackwater catchment increases of over 90 percent are found for the 50-year return period in the 2050s ~~to~~and 2080s. ~~In almost all catchments and combinations of~~ Other bias correction techniques ~~changes are greater in the~~ return more modest increases. Changes in flood

quantiles estimated using the CF and DGQM approaches show larger changes in the 2050s thanrelative to the 2080s under SSP3.in the Blackwater. Indeed, the CF method shows the most modest changes in all quantiles for the 2080s relative to other time periods across all catchments. In the Slaney most bias correction methods show only small changes in flood quantiles between time periods, the exception being EQM which shows substantial increases in each flood quantile moving across each time-period. The EQM method tends to show the greatest increases in magnitude for higher quantile floods, with largest percent changes returned for the 50-year return period. In the Newport and Boyne catchments, the CF approach shows modest reductions in the magnitude of higher frequency floods, a characteristic not reported using other bias correction techniques.

3.4 Uncertainty estimation and decomposition for flood hazardquantile estimation

The magnitude of each of the four sources of uncertainty on flood riskhazard estimation was estimated first based on the additive chain principle to reveal their contribution to the overall uncertainty in projected changes. Projections from each of 12 climate models were iteratively passed through five bias correction techniques and used to force the GR4J model using behavioural parameters sets, before fitting each of the three frequency distributions to estimate future flood hazard. Figure 12Therefore, for the spread for climate models was evaluated by varying simulations using each of the 12 GCMs while using a single bias correction technique, median hydrological model parameter set and a single flood frequency distribution. Figure 11 presents the integrative range of this cascade of uncertainty in estimating return period floods for each catchment using data spanning the years 1976-2100. The dominant source of uncertainty differs from catchment to catchment. Climate models, flood frequency distribution and bias correction techniques tend to be the dominant contributing source of uncertainty in estimating flood quantiles. InUsing this one at a time approach to evaluating uncertainties in flood quantiles, in the Newport and Blackwater catchments climate model projections present the dominant source of uncertainty, particularly for higher flood quantiles. Notably the relative magnitude of uncertainty in the smaller flood quantiles in the Blackwater catchment is different than for larger flood quantiles, with the extreme value distribution becoming dominant at lower flood quantiles. The largest source of uncertainty in the Slaney is derived from the use of different frequency distribution models. For the Boyne catchment the bias correction methods contribute more to the total uncertainty. Therefore, the various steps in the modelling chain contribute differently in each catchment to total uncertainty in future flood riskhazard estimation and in some catchments vary depending on the flood quantile of interest (Figure 1211).

While additive chains may be useful for evaluating individual components of uncertainty, they do not allow identification of the interactive components of the uncertainty cascade. We use ANOVA to decompose the contribution of individual sources of uncertainty and their interaction in contributing to the total uncertainty in future flood hazard (Figure 1312). We evaluate changes in 10-year, 50-year and 100-year return period flood for the 2080s (2070-2099) relative to the reference period (1976-2005). The decomposition of uncertainty is based on the variance in changes of flood quantile values and calculated out of 100 percent, i.e. the sum of all sources is equal to 100. The contribution of each source of uncertainty is not uniform across the selected catchments (Figure 1312). Taking the example of the magnitude of the 100 year flood (Figure 1312 outer band),

future flood hazard in the Blackwater catchment for the 2080s is highly sensitive to the climate model used (36.5% of total uncertainty in 100-year flood) and respective bias correction methods (20% of total uncertainty). By contrast, future flood frequency in the Boyne is more sensitive to bias correction methods (30.0%) and extreme value distribution (25.5%) employed. In the Boyne catchment, the climate model ensemble accounts for less than one quarter (22.5%) of the uncertainty in simulations of the 100-year flood by the 2080s and is comparable in magnitude to the interactive components of the cascade. In the Newport catchment the use of different extreme value distributions (36.3%) presents the largest component of uncertainty., followed by the climate model ensemble. The results of ANOVA analysis also confirm that the uncertainty resultant from the interaction of the key sources considered is not negligible and also varies on a catchment basis. In the Slaney and Blackwater catchments the interaction of various uncertainty components accounts for 16.8% and 16% of the total uncertainty in estimates of the 100-year flood by the 2080s. By contrast, interactive components in the Newport and Boyne catchments account for approximately one quarter of the uncertainty range (25.2% in the Newport and 22% in the Boyne). Overall, hydrological parameter uncertainty is the least dominant source of uncertainty in future flood frequency estimates across each catchment (Figure ~~12~~11 and Figure ~~13~~12). For estimates of the 100-year flood in the 2080s (Figure ~~13~~12 outer band), hydrological model parameter uncertainty is typically 5% of the total uncertainty, reaching up to 9% in the Boyne. Furthermore, the contribution of each of the main components of uncertainty and their interactions to total uncertainty is broadly similar for the different return periods considered for our analysis of the 2080s (Figure ~~13~~12).

4. Discussion

We examined future ~~flood risk~~changes in flooding for four catchments in Ireland, including within our modelling chain the uncertainties derived from 12 CMIP6 GCMs, 5 commonly used bias correction techniques, hydrological model parameters and three flood frequency distributions. We found that maximum precipitation ~~and mean air temperature~~ in all catchments ~~are~~is projected to increase over the coming decades, however changes are not uniform across catchments. The largest change in annual maximum precipitation was found for the Newport catchment, with ensemble median increases becoming progressively larger for the 2020s, 2050s and 2080s (27%, 40%, 60%, respectively). In the Slaney catchment, increases in annual maximum precipitation between the 2050s and 2080s are not statistically significant. In the Blackwater catchment, most of the climate models indicate a positive change but these have a wide range of uncertainty relative to other catchments (from 0 to 55% in 2050s and 0 to 60% in 2080s). We find projected changes in flood magnitudes to be broadly proportional to changes in maximum precipitation in all catchments. Projected changes in flood magnitude are higher using the ~~SSP1~~SSP585 and ~~SSP5~~lower using SSP126 climate scenarios~~, whereas the SSP3 results in more modest flood increases~~. Overall changes in precipitation and air temperature are broadly consistent with previous findings using CMIP5 (Broderick et al., 2019) in Ireland.

560 Our findings demonstrate the large uncertainties associated with projected flood magnitudes. with climate change. Over recent years much research has sought to explore the dominant sources of uncertainty in climate change impact assessments. For instance, Bastola et al. (2011b) identify hydrological model uncertainty as important in previous assessment of change in flood risk, others have identified climate models as being the dominant source (e.g.Similar studies have identified climate models as being the dominant source (e.g. Sulis et al., 2012; Sulis et al., 2012; Hattermann et al., 2018). Mizukami et al. (2016) rank

565 hydrological model structure of greater importance than bias correction approaches in US catchments. However, our findings call into question the ability to generalise the most important components of the cascade of uncertainty in assessing future flood risk across catchments. Using variance decomposition to partition the components of the modelling chain employed, together with their interactions, we show that the dominant sources of uncertainty in assessing climate change impacts on future floods differ on a catchment by catchment basis. In two of our study catchmentsIndeed (Addor et al. (2014)highlight

570 that there seems to be a general agreement in the literature on the dominant contribution of climate models to the uncertainty in discharge projections. On the contrary, our findings demonstrate the challenges of generalising about the dominant components of the cascade of uncertainty at the catchment scale. Using both additive chains and variance decomposition to examine components of the modelling chain employed, our results show that not only does the contribution and importance of different components of the modelling chain vary across catchments, but that the dominant source of uncertainty can be

575 completely different. Moreover, the dominant sources of uncertainty vary depending on which approach is used to evaluate uncertainty. Using additive chains, in two of our study catchments, the climate model ensemble was the dominant source of uncertainty, as was expected. However, for the other two catchments, namely the Boyne and the Slaney, the extreme value distribution employed for flood frequency analysis and the bias correction method used to adjust raw GCM output contribute greater uncertainty to future flood risk than the ensemble of GCMs employed. Across all catchments the uncertainty in future

580 hydrological model parameters is the smallest component of total uncertainty, whileUsing variance decomposition that allows for the interaction of components of the modelling chain to be evaluated and quantified offers a fuller assessment of uncertainty. Our result show that in the Slaney and Blackwater catchments the climate model ensemble used dominated the cascade of uncertainty. In the Slaney, the second most important component is the bias correction technique used, while in the Blackwater the frequency distribution model comes second. In the Newport catchment the flood frequency distribution model

585 used ranks as the most important component of the cascade of uncertainty, followed by the climate model ensemble. Finally, in Boyne catchment, the climate model ensemble ranks as only the third most important component of the uncertainty cascade in simulating flood quantiles, with the bias correction methods coming first and the flood frequency distribution second.

We hypothesise how catchment characteristics may influence the dominant components of the cascade of uncertainty in each

590 catchment. The Slaney and Blackwater where climate models dominate are among the largest in our sample with groundwater contributing significantly to runoff in both. In the Blackwater catchment topography has a large bearing on flood response time within the catchment with flood peaks moving more rapidly from elevated sub-catchments into the main channel and may be a reason as to why the flood frequency model ranks as the second dominant component in the cascade of uncertainty. The

Slaney catchment drains the southern component of the Wicklow mountains before reaching shallower elevations as it flows south through Carlow and Wexford. The variation in topography and hence precipitation from upper to lower reaches may be a reason as to why bias correction methods emerge as the second most important component of the uncertainty cascade in this catchment. The Newport catchment is the smallest in our sample with flood response influenced more strongly by varied land use cover (forestry) and the presence of a lake in the upper reaches of the catchment. The flood frequency distribution dominates the cascade, followed by the climate model ensemble used. Finally, the Boyne catchment has been heavily influenced by arterial drainage works, resulting in the insertion of field drains and the deepening and widening of the river channel (Harrigan et al., 2014). These interventions have resulted in a faster rainfall runoff response. In the Boyne catchment therefore, projected changes in future rainfall are likely to have a more direct bearing on the flood response, with uncertainty in bias correction and the flood frequency distribution dominating the cascade of uncertainty.

Across each of our catchments and in the context of the modelling chain employed, the uncertainty from hydrological model parameters is the smallest component of total uncertainty in the estimation of future flood hazard magnitude. Bastola et al. (2011a; 2011 b) identify hydrological model uncertainty as important in a previous assessment of change in flood risk, while Mizukami et al. (2016) rank hydrological model uncertainty of greater importance than bias correction approaches in US catchments. We note that we do not consider hydrological model structure uncertainty in our modelling chain and that our decision to select only the top 300 behavioural parameter sets, rather than all those identified may be a factor here. This highlights how subjective decisions in the application of hydrological models may have important implications for the uncertainty in future projections (Melsen et al., 2019). We also find that the contribution to total uncertainty from the interaction of components within the modelling chain is substantial – up to one quarter of the uncertainty range considered in two catchments.

While our sample is small, results suggest that rather than being the same across catchments, the dominant sources of uncertainty in future flood quantiles are catchment dependent. While uncertainty decomposition may be useful in helping scientists navigate the cascade of uncertainty by prioritising the key components of the uncertainty cascade to sample (Clark et al., 2016) for a particular catchment, our small sample makes it difficult to determine how catchment characteristics may be informative in identifying the dominant sources of uncertainty a priori. There are some indications that catchment properties and the characteristics of observed precipitation may influence which uncertainties may dominate. Vetter et al. (2017) used variance decomposition to examine the contribution of modelling chains (GCM, emissions scenario (in the form of Representative Concentration Pathways (RCPs)) and hydrological model) to total uncertainty in different parts of the flow regime. In their study they examine 12 large catchments globally. While Vetter et al. (2017) highlight the dominance of GCMs in total uncertainty across many catchments they highlight that the share of emissions scenario and hydrological model contributions to overall uncertainty can differ between catchments. Similar to our findings, Vetter et al. (2017) highlight the importance of interacting components of the modelling chain employed. The possibility that dominant sources of uncertainty

differ on a catchment by catchment basis presents challenges for both top down and bottom up approaches to climate change adaptation. Top down approaches must a priori decide on the components of the modelling chain to include. Including all relevant components is a very resource expensive task (Smith et al., 2018) and it may not be apparent at the outset which components of modelling chain to include for specific catchments. For bottom up approaches, such as the scenario neutral method (Broderick et al., 2019), the modeller is forced to choose which aspects of uncertainty to prioritise in assessing sensitivity to future changes. Again, this may not be apparent a priori. Moreover, the findings of Dobler et al. (2012) suggest that the dominant components of the modelling chain may further vary depending on which part of the flow regime (low, mean, high flows) is of interest. They highlight, for example, that the importance of bias correction approaches to the overall uncertainty in hydrological response increases for high flows. Our analysis of flood magnitudes for different return periods using all data from 1976-2100 suggests that the dominant source of uncertainty may also vary based on the return period of interest.

Our results show the value of ANOVA based methods for examining and visualising the relative contribution of uncertainties within the modelling chain considered. In our example we used the planning horizon of the 2080s to decompose uncertainties. In addition, the use of ANOVA techniques to quantify uncertainty may offer insight into where effort to reduce uncertainty may be most fruitful (Clark et al., 2016). In all catchments the magnitude of change in flood events is heavily dependent on the approach to bias correction. Across all catchments EQM performs the poorest at matching precipitation quantiles during the historical period. All other methods considered show consistent performance except in the Blackwater catchment. This is likely due to long positive tail of the precipitation distribution and intensity characteristics in the Blackwater. On the whole, distribution based methods tend to be most consistent across the selected catchments and also have relatively smaller spread. Therefore, the DGQM or SGQM method (s) are promising for future risk evaluation and minimizing uncertainty.

Given the importance of uncertainty quantification in adapting to climate change it should be a priority for future work to examine how the dominant components of uncertainty in modelling chains relate to catchment characteristics. While our study of four catchments is limited in this regard, there is evidence that catchment characteristics, which provide insight into the processes governing the rainfall runoff response, may also play a role in determining the components of the modelling chain that dominate uncertainties in future flood projections. The Newport catchment is the smallest of our sample (146 Km²) and is an elevated catchment with a flashy response to rainfall. The shorter time of concentration and linear precipitation runoff relationship mean that this catchment is highly sensitive to changes in extreme precipitation with uncertainty in flood frequency distribution and bias correction accounting for over half of the total uncertainty in the projected 100 year flood in the 2080s. The Boyne catchment has been subject to significant arterial drainage works which have resulted in a faster rainfall runoff response and elevated high flows (Harrigan et al., 2020; Berghuijs et al., 2019). Our findings suggest that bias correction and flood frequency distribution are the dominant sources of uncertainty in the projected 100 year flood by the 2080s in this catchment. In the Blackwater and Slaney catchments groundwater contributes significantly to runoff and the catchments are

larger with typically well drained soils. In both catchments the climate model ensemble represents the dominant source of uncertainty.

665 As our study has shown, the evaluation of uncertainties and their interaction in future flood risk assessment with climate change is a critical step in understanding future impacts and informing adaptation decision making. However, results depend on the modelling chain employed. The work presented here is illustrative rather than exhaustive. We do not, for example, include uncertainties in future flood estimates derived from different hydrological model structures, nor do we evaluate the transferability of parameter sets to represent future rainfall runoff response (e.g. Broderick et al. 2016). We also assume that

670 flood processes remain stationary within the 30-year windows used to evaluate changes, while we also assume that other factors that can influence rainfall runoff response, such as land use change, remain unchanged from the calibration period used to train our hydrological models.

5. Conclusions

675 This study evaluates changes in future flood magnitude with climate change for four Irish catchments using a modelling chain incorporating 12 GCMs comprising the CMIP6 ensemble, 5 bias correction techniques, hydrological model parameter uncertainty and the use of extreme value distributions. Our findings suggest increasing flood risk

As our study has shown, the evaluation of uncertainties and their interaction in future flood risk assessment with climate change is a critical step in understanding future impacts and informing adaptation decision making. However, results depend on the

680 modelling chain employed and the method used to quantify uncertainties. Given the possibility of examining interactive components of modelling chain, we recommend the use of ANOVA based techniques to decompose the cascade of uncertainty. We highlight however that our modelling chain is not complete and that the work presented here is illustrative rather than exhaustive. We do not, for example, include uncertainties in future flood estimates derived from different hydrological model structures with previous work, as indicated above, showing that hydrological model structure and complexity may be an

685 important component of future uncertainties. Other potential sources of hydrological model uncertainty are also omitted. For example, we did not evaluate the transferability of parameter sets to represent future rainfall runoff response (e.g. Broderick et al. 2016), nor did we evaluate the influence that selection of different objective functions may have on the identification of behavioural parameter sets. Westerberg et al. (2020) also highlight the potential importance of uncertainty in the discharge data used to calibrate hydrological models. In assessing different flood quantiles, we use only 30 years of annual maxima to

690 extrapolate to return periods outside our record length. Such extrapolations should be treated cautiously but are prevalent in many studies (e.g. Alison L. Kay et al., 2006; Lawrence, 2020; Meresa and Romanowicz, 2017) while rarer floods are also associated with design standards (e.g. 100-year flood) and therefore of interest to decision makers. We also assume that flood processes remain stationary within the 30-year windows used to evaluate changes, while other factors that can influence rainfall runoff response, such as land use change, remain unchanged from the calibration period used to train our hydrological models.

695

5. Conclusions

This study evaluates changes in future flood magnitude with climate change for four Irish catchments using a modelling chain incorporating 12 GCMs comprising the CMIP6 ensemble, 5 bias correction techniques, hydrological model parameter uncertainty and the use of extreme value distributions. Our findings suggest increasing flood hazards over the coming decades in all catchments, with changes in flooding largely consistent with changes in maximum precipitation. However, uncertainties in future flood changes are large and increase with time and flood quantile. Using ANOVA, we decompose uncertainties in future flood quantiles to examine how individual components of the~~the~~our modelling chain and their interactions contribute to overall uncertainty. Our results show ~~that~~how the dominant sources of uncertainty may vary on a catchment basis, ~~calling into question~~highlighting the ~~ability~~inability to generalise on the dominant components of uncertainty across catchments~~, even in a relatively small domain like Ireland.~~. Across all four catchments the climate models, bias ~~correlation~~correction methods and the extreme value distributions used to evaluate flood return periods were differentially dominant, while the uncertainty derived from the interaction of various components was substantial in all catchments. ~~Hydrological model parameter uncertainty was the least important component.~~ Our work shows the value of ANOVA methods in visualising and quantifying the uncertainty cascade at a catchment level which will be helpful in navigating the uncertainties associated with future flood risk for better adaptation decision making. While our sample is small, ~~there is evidence that~~ the dominant components of uncertainty in future flood risk may be related to catchment characteristics. ~~Future~~We therefore recommend that future work seeks to better understand the link between the key components of the cascade of uncertainty and catchment characteristics ~~is therefore recommended.~~. Ability to do so would offer considerable advantages in knowing a-priori which sources of uncertainty should be targeted as priority.

Acknowledgements

We thank data providers and three reviewers for their constructive comments and feedback which helped improve our manuscript.

Funding

This work was made possible by the award of funding from the Office of Public Works and Kildare County Council to HM, CM and RF.

Conflict of interest

None

References

730

Addor, N., O. Rossler, N. K € oplin, M. €, Huss, R. Weingartner, and J. S., & (2014). (2014). Water Resources Research. *Robust Changes and Sources of Projected, Uncertainty in the Swiss, Hydrological Regimes of Catchments, Water Resour. Res., 50 7541–7562, Doi:10.1002/ 2014WR015549*, 5375–5377. https://doi.org/10.1002/2013WR014979.Reply

Bastola, S., Murphy, C., and& Sweeney, J.... (2011a). The role of hydrological modelling uncertainties in climate change impact assessments of Irish river catchments. *Advances in Water Resources*, *34*(5), 562–576. https://doi.org/10.1016/j.advwatres.2011.01.008, 2011a.

Bastola, S., Murphy, C., and& Sweeney, J.:. (2011b). The sensitivity of fluvial flood risk in Irish catchments to the range of IPCC AR4 climate change scenarios. *Science of the Total Environment*, *409*(24), 5403–5415. https://doi.org/10.1016/j.scitotenv.2011.08.042, 2011b.

Berg, P., Feldmann, H., and Panitz, H. J:. Bias correction of high resolution regional climate model data. Journal of Hydrology, 448–449, 80–92. https://doi.org/10.1016/j.jhydrol.2012.04.026, (2012).

Berghuijs, W. R., Harrigan, S., Molnar, P., Slater, L. J., and Kirchner, J. W:. The Relative Importance of Different Flood-Generating Mechanisms Across Europe. Water Resources Research, 55(6), 4582–4593. https://doi.org/10.1029/2019WR024841, (2019).

Beven, K., and& Binley, A.:. (1992). The future of distributed models: Model calibration and uncertainty prediction. *Hydrological Processes*, *6*(3), 279–298. https://doi.org/10.1002/hyp.3360060305, (1992).

Blöschl, G., Bierkens, M. F. P., Chambel, A., Cudennec, C., Destouni, G., Fiori, A., Kirchner, J. W., McDonnell, J. J., Savenije, H. H. G., Sivapalan, M., Stumpp, C., Toth, E., Volpi, E., Carr, G., Lupton, C., Salinas, J., Széles, B., Viglione, A., Aksoy, H., … Zhang, Y. (2019). Twenty-three unsolved problems in hydrology (UPH)–a community perspective. *Hydrological Sciences Journal*, *64*(10), 1141–1158. https://doi.org/10.1080/02626667.2019.1620507

Blöschl, G., Hall, J., Parajka, J., Perdigão, R. A. P., Merz, B., Arheimer, B., Aronica, G. T., Bilibashi, A., Bonacci, O., Borga, M., Čanjevac, I., Castellarin, A., Chirico, G. B., Claps, P., Fiala, K., Frolova, N., Gorbachova, L., Gül, A., Hannaford, J., … Živković, N.:. (2017). Changing climate shifts timing of European floods. *Science*, *357*(6351), 588–590. https://doi.org/10.1126/science.aan2506, 2017.

Blöschl, G., Hall, J., Viglione, A., Perdigão, R. A. P., Parajka, J., Merz, B., Lun, D., Arheimer, B., Aronica, G. T., Bilibashi, A., Boháč, M., Bonacci, O., Borga, M., Čanjevac, I., Castellarin, A., Chirico, G. B., Claps, P., Frolova, N., Ganora, D., … Živković, N:. Changing climate both increases and decreases European river floods. Nature, 573(7772), 108–111. https://doi.org/10.1038/s41586-019-1495-6, (2019).

Broderick, C., Murphy, C., Wilby, R. L., Matthews, T., Prudhomme, C., and& Adamson, M.:. (2019). Using a Scenario-Neutral Framework to Avoid Potential Maladaptation to Future Flood Risk. *Water Resources Research*. https://doi.org/10.1029/2018WR023623, (2019).

Broderick, C., ~~Murphy, C., Mooney, P.,~~T. Matthews, ~~T:. Changes in precipitation extremes for Ireland: Theoretical basis~~R. L. Wilby, S. Bastola, and ~~future outlook. National Hydrology Conference,~~ C. Murphy (2016~~.~~), Transferability of hydrological models and ensemble averaging methods between contrasting climatic periods, Water Resour. Res., 52, 8343–8373, doi:10.1002/2016WR018850

Chen, J., Brissette, F. P., Chaumont, D., ~~and~~& Braun, M~~:.~~. (2013). Finding appropriate bias correction methods in downscaling precipitation for hydrologic impact studies over North America. *Water Resources Research*, *49*(7), 4187–4205. https://doi.org/10.1002/wrcr.20331~~, 2013.~~

Chen, L., Singh, V. P., Shenglian, G., Hao, Z., ~~and~~& Li, T~~:.~~. (2012). Flood Coincidence Risk Analysis Using Multivariate Copula Functions. *Journal of Hydrologic Engineering*, *17*(6), 742–755. https://doi.org/10.1061/(ASCE)HE.1943-5584.0000504~~, 2012.~~

Ciaran Broderick, Tom Matthews, Robert L. Wilby, Satish Bastola, and C. M. (1969). Water Resources Research. *Journal of the American Water Resources Association*, *5*(3), 2–2. https://doi.org/10.1111/j.1752-1688.1969.tb04897.x

Clark, M. P., Wilby, R. L., Gutmann, E. D., Vano, J. A., Gangopadhyay, S., Wood, A. W., Fowler, H. J., Prudhomme, C., Arnold, J. R., ~~and~~& Brekke, L. D~~:.~~. (2016). Characterizing Uncertainty of the Hydrologic Impacts of Climate Change. *Current Climate Change Reports*, *2*(2), 55–64. https://doi.org/10.1007/s40641-016-0034-x~~, 2016.~~

Dobler, C., Hagemann, S., Wilby, R. L., ~~and~~& StÃtter, J~~:.~~. (2012). Quantifying different sources of uncertainty in hydrological projections in an Alpine watershed. *Hydrology and Earth System Sciences*, *16*(11), 4343–4360. https://doi.org/10.5194/hess-16-4343-2012~~, 2012.~~

Ehret, U., Zehe, E., Wulfmeyer, V., Warrach-Sagi, K., ~~and~~& Liebert, J~~:.~~. (2012). HESS Opinions "should we apply bias correction to global and regional climate model data?" *Hydrology and Earth System Sciences*, *16*(9), 3391–3404. https://doi.org/10.5194/hess-16-3391-2012~~, 2012.~~

Fowler, H. J., Ekström, M., Blenkinsop, S., ~~and~~& Smith, A. P~~:.~~. (2007). Estimating change in extreme European precipitation using a multimodel ensemble. *Journal of Geophysical Research Atmospheres*, *112*(18). https://doi.org/10.1029/2007JD008619~~, , 2007.~~

~~Giorgi~~GIORGI, F., ~~and Gao~~& GAO, X. J~~:.~~. (2018). Regional earth system modeling: review and future directions. *Atmospheric and Oceanic Science Letters*, *11*(2), 189–197. https://doi.org/10.1080/16742834.2018.1452520~~, (2018).~~

Giuntoli, I., Villarini, G., Prudhomme, C., & Hannah, D. M. (2018). Uncertainties in projected runoff over the conterminous United States. *Climatic Change*, *150*(3–4), 149–162. https://doi.org/10.1007/s10584-018-2280-5

Gosling, S. N., Taylor, R. G., Arnell, N. W., & Todd, M. C. (2011). A comparative analysis of projected impacts of climate change on river runoff from global and catchment-scale hydrological models. *Hydrology and Earth System Sciences*, *15*(1), 279–294. https://doi.org/10.5194/hess-15-279-2011

Griffis, V. W., ~~and~~& Stedinger, J. R~~:.~~. (2007). *Evolution of Flood Frequency Analysis with Bulletin 17*. *June*, 283–297~~, 2007.~~

Gudmundsson, L., Wagener, T., Tallaksen, L. M., ~~and~~& Engeland, K~~:.~~. (2012). Evaluation of nine large-scale hydrological models with respect to the seasonal runoff climatology in Europe. *Water Resources Research*, *48*(11).

https://doi.org/10.1029/2011WR010911, 2012.

Gutjahr, O., and& Heinemann, G.,. (2013). Comparing precipitation bias correction methods for high-resolution regional climate simulations using COSMO-CLM: Effects on extreme values and climate change signal. *Theoretical and Applied Climatology*, *1*14(3–4), 511–529. https://doi.org/10.1007/s00704-013-0834-z, 2013.

Gutmann, E. Pruitt, T. Clark, MP. Brekke, L. Arnold, JR. Raff, DA. and Rasmussen RM:. An intercomparison of statistical downscaling methods used for water resources assessments in the United States. Water Resour Res 50:7167–7186. doi:10.1002/ 2014WR015559, 2014.

Hamon, W. R.,. (1964). Computation of direct runoff amounts from storm rainfall. In *General Assembly of Berkeley, Symposium on Surface Waters: Vol. Extract of* (pp. 52–62), 1964.).

Harrigan, S., Zoster, E., Cloke, H., Salamon, P., and Prudhomme, C. Daily ensemble river discharge reforecasts and real-time forecasts from the operational Global Flood Awareness System. October, 1–22, 2020.

Harrigan, S., Murphy, C., Hall, J., Wilby, R. L., & Sweeney, J. (2014). Attribution of detected changes in streamflow using multiple working hypotheses. *Hydrology and Earth System Sciences*, *18*(5), 1935–1952. https://doi.org/10.5194/hess-18-1935-2014

Hattermann, F. F., Vetter, T., Breuer, L., Su, B., Daggupati, P., Donnelly, C., Fekete, B., Florke, F., Gosling, S. N., Hoffmann, P., Liersch, S., Masaki, Y., Motovilov, Y., Muller, C., Samaniego, L., Stacke, T., Wada, Y., Yang, T., and& Krysnaova, V.,. (2018). Sources of uncertainty in hydrological climate impact assessment: A cross-scale study. *Environmental Research Letters*, *13*(1). https://doi.org/10.1088/1748-9326/aa9938, 2018.

He, S., Guo, S., Liu, Z., Yin, J., Chen, K., and& Wu, X.,. (2018). Uncertainty analysis of hydrological multi-model ensembles based on CBP-BMA method. *Hydrology Research*, *49*(5), 1636–1651. https://doi.org/10.2166/nh.2018.160, 2018.

Hughes, D. A., Kingston, D. G., & Todd, M. C.,. (2011). Uncertainty in water resources availability in the Okavango River basin as a result of climate change. *Hydrology and Earth System Sciences*, *15*(3), 931–941. https://doi.org/10.5194/hess-15-931-2011, 2011.

Iternational Panel on Climate Change (IPCC):.IPCC. (2013). IPCC CLIMATE CHANGE 2013 Climate Change 2013. In *Researchgate.Net*. https://doi.org/10.1017/CBO9781107415324.Summary, 2013.

Jobst, A. M., Kingston, D. G., Cullen, N. J., & Schmid, J. (2018). Intercomparison of different uncertainty sources in hydrological climate change projections for an alpine catchment (upper Clutha River, New Zealand). *Hydrology and Earth System Sciences*, *22*(6), 3125–3142. https://doi.org/10.5194/hess-22-3125-2018

Kay, A. L., Davies, H. N., Bell, V. A., and& Jones, R. G.,. (2009). Comparison of uncertainty sources for climate change impacts: Flood frequency in England. *Climatic Change*, *92*(1–2), 41–63. https://doi.org/10.1007/s10584-008-9471-4, 2009.

Kay, Alison L., Jones, R. G., & Reynard, N. S. (2006). RCM rainfall for UK flood frequency estimation. II. Climate change results. *Journal of Hydrology*, *318*(1–4), 163–172. https://doi.org/10.1016/j.jhydrol.2005.06.013

Knutti, R., and& Sedláček, J.,. (2013). Robustness and uncertainties in the new CMIP5 climate model projections. *Nature*

Climate Change, *3*(4), 369–373. https://doi.org/10.1038/nclimate1716~~, 2013~~.

Krinner, G., ~~and~~& Flanner, M. G~~.~~. (2018). Striking stationarity of large-scale climate model bias patterns under strong climate change. *Proceedings of the National Academy of Sciences of the United States of America*, *115*(38), 9462–9466. https://doi.org/10.1073/pnas.1807912115~~, 2018~~.

Lafon, T., Dadson, S., Buys, G., ~~and~~& Prudhomme, C~~.~~. (2013). Bias correction of daily precipitation simulated by a regional climate model: A comparison of methods. *International Journal of Climatology*, *33*(6), 1367–1381. https://doi.org/10.1002/joc.3518~~, 2013~~.

Lawrence, D~~.~~. (2020). Uncertainty introduced by flood frequency analysis in projections for changes in flood magnitudes under a future climate in Norway. *Journal of Hydrology: Regional Studies*, *28*(December 2019), 100675. https://doi.org/10.1016/j.ejrh.2020.100675~~, 2020~~.

Li, L., Xu, C. Y., Xia, J., Engeland, K., ~~and~~& Reggiani, P~~.~~. (2011). Uncertainty estimates by Bayesian method with likelihood of AR (1) plus Normal model and AR (1) plus Multi-Normal model in different time-scales hydrological models. *Journal of Hydrology*, *406*(1–2), 54–65. https://doi.org/10.1016/j.jhydrol.2011.05.052~~, 2011~~.

Mazzorana, B., Levaggi, L., Keiler, M., ~~and~~& Fuchs, S~~.~~. (2012). Towards dynamics in flood risk assessment. *Natural Hazards and Earth System Science*, *12*(11), 3571–3587. https://doi.org/10.5194/nhess-12-3571-2012~~, 2012~~.

Melsen, L. A., Teuling, A. J., Torfs, P. J. J. F., Zappa, M., Mizukami, N., Mendoza, P. A., Clark, M. P., ~~and~~& Uijlenhoet, R~~.~~. (2019). Subjective modeling decisions can significantly impact the simulation of flood and drought events. *Journal of Hydrology*, *568*(November 2018), 1093–1104. https://doi.org/10.1016/j.jhydrol.2018.11.046~~, 2019~~.

Meresa, H.K., ~~and~~& Romanowicz, R. J~~.~~. (2017). The critical role of uncertainty in projections of hydrological extremes. *Hydrology and Earth System Sciences*, *21*(8). https://doi.org/10.5194/hess-21-4245-2017~~, 2017~~.

Meresa, Hadush K., ~~and~~& Gatachew, M. T~~.~~. (2019). Climate change impact on river flow extremes in the upper blue nile river basin. *Journal of Water and Climate Change*, *10*(4), 759–781. https://doi.org/10.2166/wcc.2018.154~~, 2019~~.

Meresa, ~~H~~Hadush K., ~~and~~& Romanowicz, R. J~~.~~. (2017). The critical role of uncertainty in projections of hydrological extremes. *Hydrology and Earth System Sciences*. https://doi.org/10.5194/hess-21-4245-2017~~, 2017~~.

Meresa, ~~H~~Hadush K, Romanowicz, R. J., ~~and~~& Napiorkowski, J. J~~.~~. (2017). Understanding changes and trends in projected hydroclimatic indices in selected Norwegian and Polish catchments. *Acta Geophysica*, *65*(4), 829–848. https://doi.org/10.1007/s11600-017-0062-5~~, 2017~~.

Meresa, ~~H K.:~~Hadush Kidane. (2020). River flow characteristics and changes under the influence of varying climate conditions. *Natural Resource Modeling*, *33*(1), 1–30. https://doi.org/10.1111/nrm.12242~~, 2020~~.

Mizukami, N., Clark, M. P., Gutmann, E. D., Mendoza, P. A., Newman, A. J., Nijssen, B., Livneh, B., Hay, L. E., Arnold, J. R., ~~and~~& Brekke, L. D~~.~~. (2016). Implications of the methodological choices for hydrologic portrayals of climate change over the contiguous united states: Statistically downscaled forcing data and hydrologic models. *Journal of Hydrometeorology*, *17*(1), 73–98. https://doi.org/10.1175/JHM-D-14-0187.1~~, 2016~~.

~~Osuch, M., Romanowicz, R. J., Lawrence, D., and Wong, W. K.:~~Osuch, M., Lawrence, D., Meresa, H. K., Napiorkowski, J.

J., & Romanowicz, R. J. (2017). Projected changes in flood indices in selected catchments in Poland in the 21st century. *Stochastic Environmental Research and Risk Assessment, 31*(9). https://doi.org/10.1007/s00477-016-1296-5

Osuch, M., Romanowicz, R. J., Lawrence, D., & Wong, W. K. (2015). Assessment of the influence of bias correction on meteorological drought projections for Poland. *Hydrology and Earth System Sciences Discussions, 12*(10), 10331–10377. https://doi.org/10.5194/hessd-12-10331-2015, 2015.

Osuch, Marzena, Romanowicz, R. J., Lawrence, D., and& Wong, W. K:.. (2016). Trends in projections of standardized precipitation indices in a future climate in Poland. *Hydrology and Earth System Sciences, 20*(5), 1947–1969. https://doi.org/10.5194/hess-20-1947-2016, 2016.

Peleg, N., Shamir, E., Georgakakos, K. P., & Morin, E. (2015). *A framework for assessing hydrological regime sensitivity to climate change in a convective rainfall environment : a case study of two medium-sized eastern Mediterranean catchments , Israel. 2*, 567–581. https://doi.org/10.5194/hess-19-567-2015

Perrin, C., Michel, C., and& Andréassian, V:.. (2003). Improvement of a parsimonious model for streamflow simulation. *Journal of Hydrology, 279*(1–4), 275–289. https://doi.org/10.1016/S0022-1694(03)00225-7, 2003.

Piani, C., Haerter, J. O., and& Coppola, E:.. (2010). Statistical bias correction for daily precipitation in regional climate models over Europe. *Theoretical and Applied Climatology, 99*(1–2), 187–192. https://doi.org/10.1007/s00704-009-0134-9, 2010.

Prudhomme, C., Parry, S., Hannaford, J., Clark, D. B., Hagemann, S., and& Voss, F:.. (2011). How well do large-scale models reproduce regional hydrological extremes: In Europe? *Journal of Hydrometeorology, 12*(6), 1181–1204. https://doi.org/10.1175/2011JHM1387.1, 2011.

Raff, D. A., & Rasmussen, R. M. (2014). *used for water resource assessments in the United States. 7167–7186.* https://doi.org/10.1002/2014WR015559.Received

Rojas, R., Feyen, L., and& Watkiss, P. (2013). Climate change and river floods in the European Union: Socio-economic consequences and the costs and benefits of adaptation. *Global Environmental Change, 23*(6), 1737–1751. https://doi.org/10.1016/j.gloenvcha.2013.08.006, 2013.

Saini, R., Wang, G., Yu, M., and& Kim, J:.. (2015). Phytoplankton light absorption and the package effect in relation to photosynthetic and photoprotective pigments in the northern tip of Antarctic Peninsula. *Journal of Geophical Research,* 3679–3699. https://doi.org/10.1002/2014JD022599, 2015.Received

Shepherd, T. G., Boyd, E., Calel, R. A., Chapman, S. C., Dessai, S., Dima-west, I. M., Fowler, H. J., & James, R. (2018). *Storylines : an alternative approach to representing uncertainty in physical aspects of climate change. 555–571.*

Smith, K. A., Wilby, R. L., Broderick, C., Prudhomme, C., Matthews, T., Harrigan, S., and& Murphy, C:.. (2018). Navigating Cascades of Uncertainty — As Easy as ABC? Not Quite…. *Journal of Extreme Events, 05*(01), 1850007. https://doi.org/10.1142/s2345737618500070, 2018.

Soriano, E., Mediero, L., and& Garijo, C:.. (2019). Selection of bias correction methods to assess the impact of climate change on flood frequency curves. *Water (Switzerland), 11*(11). https://doi.org/10.3390/w11112266, 2019.

Steele-Dunne, S., Lynch, P., McGrath, R., Semmler, T., Wang, S., Hanafin, J., and Nolan, P:. The impacts of climate change on hydrology in Ireland. Journal of Hydrology, 356(1–2), 28–45. https://doi.org/10.1016/j.jhydrol.2008.03.025, 2008.

Sulis, M., Paniconi, C., Marrocu, M., Huard, D., and& Chaumont, D:.. (2012). Hydrologic response to multimodel climate output using a physically based model of groundwater/surface water interactions. *Water Resources Research*, *48*(12), 1–18. https://doi.org/10.1029/2012WR012304, 2012.

Teng, J., Vaze, J., Chiew, F. H. S., Wang, B., and& Perraud, J. M. (2012). Estimating the relative uncertainties sourced from GCMs and hydrological models in modeling climate change impact on runoff. *Journal of Hydrometeorology*, *13*(1), 122–139. https://doi.org/10.1175/JHM-D-11-058.1, 2012.

Teutschbein, C., and& Seibert, J:.. (2013). Is bias correction of regional climate model (RCM) simulations possible for non-stationary conditions. *Hydrology and Earth System Sciences*, *17*(12), 5061–5077. https://doi.org/10.5194/hess-17-5061-2013, 2013.

Vetter, T., Reinhardt, J., Flörke, M., Griensven, A. Van, Hattermann, F., Seidou, O., Su, B., and& Vervoort, R. W:.. (2016). Evaluation of sources of uncertainty in projected hydrological changes under climate change in 12 large-scale river basins. *Climatic Change*. https://doi.org/10.1007/s10584-016-1794-y, 2016.

Vetter, T., Reinhardt, J., Flörke, M., van Griensven, A., Hattermann, F., Huang, S., Koch, H., Pechlivanidis, I. G., Plötner, S., Seidou, O., Su, B., Vervoort, R. W., and& Krysanova, V:.. (2017). Evaluation of sources of uncertainty in projected hydrological changes under climate change in 12 large-scale river basins. *Climatic Change*, *141*(3), 419–433. https://doi.org/10.1007/s10584-016-1794-y, 2017.

Walsh, S:.. (2012). a Summary of Climate Averages. *The Irish Meteorological Service*, *582*(417). www.met.ie, 2012.

Westerberg, I. K., Sikorska-Senoner, A. E., Viviroli, D., Vis, M., & Seibert, J. (2020). Hydrological model calibration with uncertain discharge data. *Hydrological Sciences Journal*, *0*(0). https://doi.org/10.1080/02626667.2020.1735638

Wilby, R. L., and& Harris, I:.. (2006). A framework for assessing uncertainties in climate change impacts: Low-flow scenarios for the River Thames, UK. *Water Resources Research*, *42*(2), 1–10. https://doi.org/10.1029/2005WR004065, 2006.

Wilby, R., Murphy, C., Wilby, R., and& Murphy, C:.. (2019). Decision-Making by Water Managers Despite Climate Uncertainty. In *The Oxford Handbook of Planning for Climate Change Hazards* (Issue February). https://doi.org/10.1093/oxfordhb/9780190455811.013.52, 2019.

Wilby, R.L. and Dessai, S:. Robust adaptation to climate change. Weather, 65(7), pp.180-185, 2010.

Wyser, K., van Noije, T., Yang, S., von Hardenberg, J., O'Donnell, D., and& Döscher, R. (2019). On the increased climate sensitivity in the EC-Earth model from CMIP5 to CMIP6. *Geoscientific Model Development Discussions*, *November*, 1–13. https://doi.org/10.5194/gmd-2019-282, 2019.

Xu, L. L. C:.. (2014). *The comparison of sensitivity analysis of hydrological uncertainty estimates by GLUE and Bayesian method under the impact of precipitation errors*. 491–504. https://doi.org/10.1007/s00477-013-0767-1, 2014.

Yang, W., Andréasson, J., Graham, L. P., Olsson, J., Rosberg, J., and& Wetterhall, F. (2010). Distribution-based scaling to improve usability of regional climate model projections for hydrological climate change impacts studies. *Hydrology*

Research, *41*(3–4), 211–229. https://doi.org/10.2166/nh.2010.004, 2010.

935

940

945
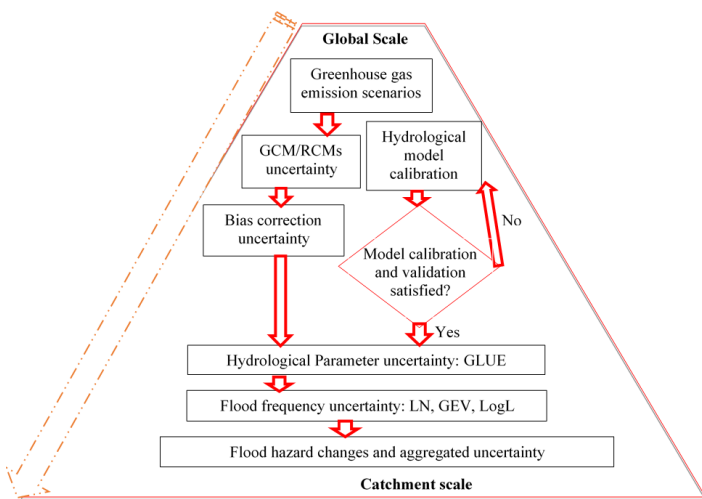
950 **Figure 1.** Research flow chart to estimate projections of flood hazard and identify associated uncertainty
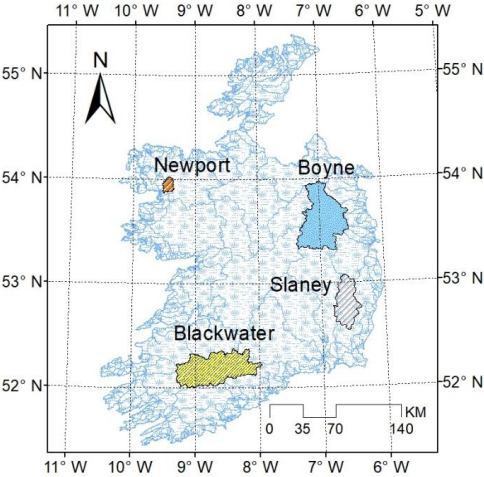
Figure 2. Location of the selected study catchments.

955
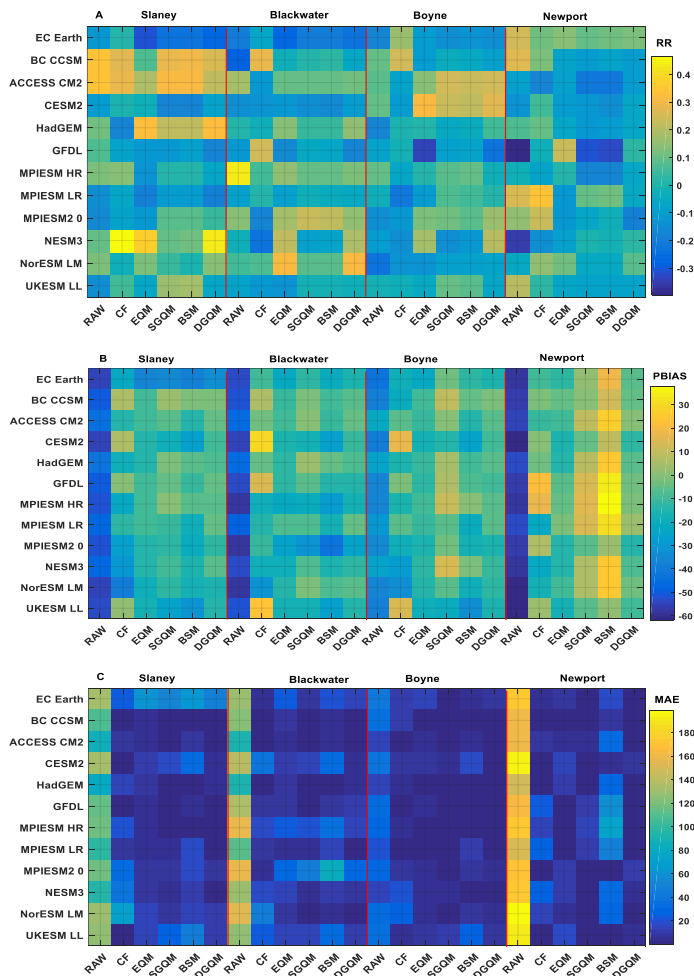
Figure 3 Comparison of corrected annual maximum daily precipitation using five bias correction methods and observed annual maximum precipitation using a) Pearson correlation coefficient (RR), b) Percent Bias (PBIAS) and c) Mean Absolute Error (MAE). The y-axis indicates each of 12 CMIP6 climate models and the x-axis represents each of 5 climate bias correction method.

965
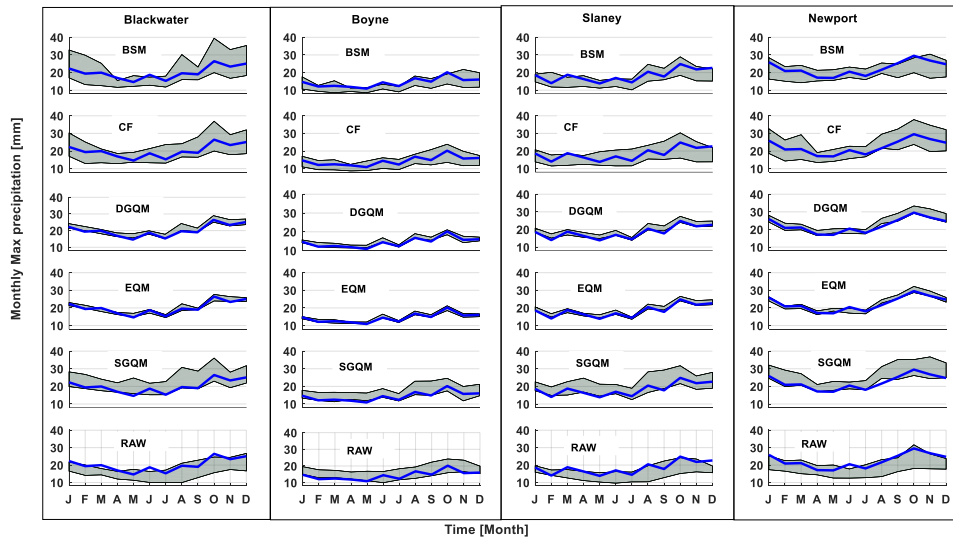
Figure 4 Comparison of raw and bias corrected simulations from 12 CMIP6 GCMs with observed ~~monthly~~ maximum daily precipitation in each month for each of our four study catchments. Each row presents results of one of five bias correction techniques (top row - Birnbaum Distribution (BSM), second row-Change Factors (CF), third row- Double Quantile Mapping
970 using Gamma Distribution (DGQM), fourth row-Empirical Quantile Mapping using Simple Interpolation (EQM), fifth row-Single Quantile Mapping using Gamma Distribution (SGQM), and the last row is the raw GCMs output). In each panel the grey shaded region represents the spread of 12 GCM simulations, with blue line being the observed ~~monthly~~ maximum precipitation.

975
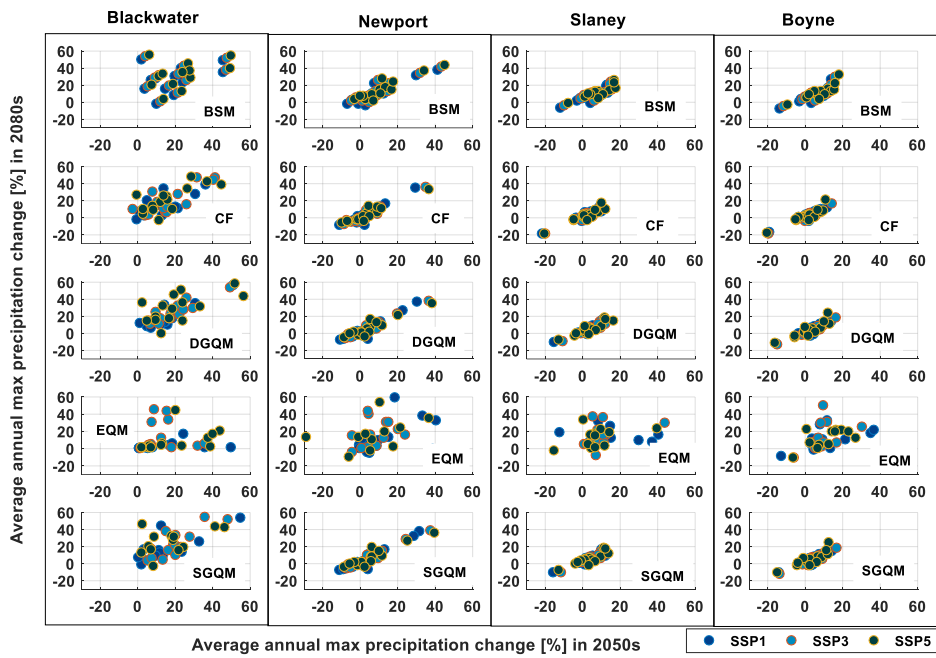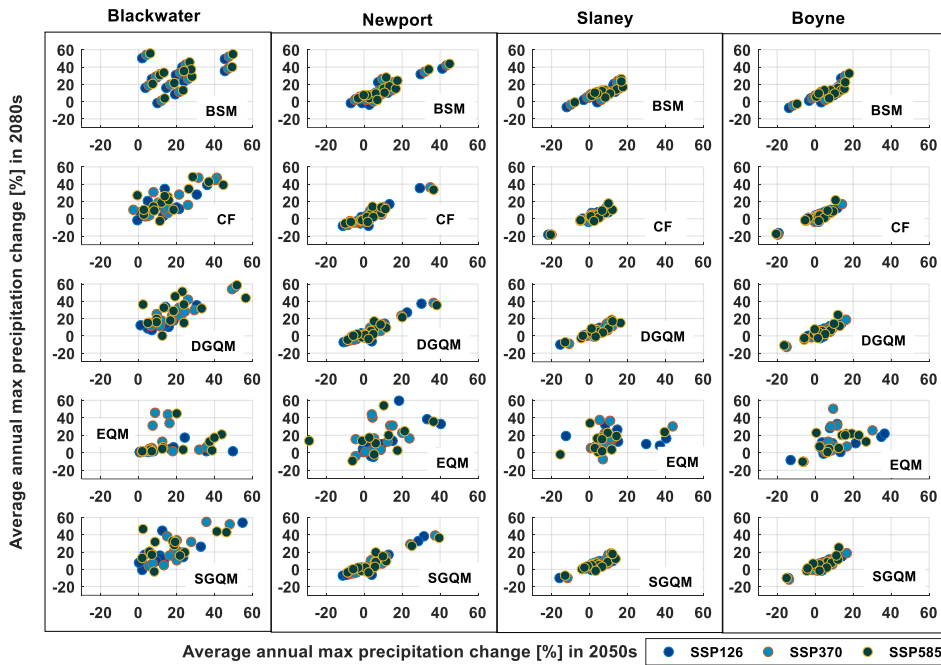
Figure 5. Scatter plots of change in maximum annual ~~daily~~ _daily_ precipitation as simulated by 12 CMIP6 GCMs (each ~~circle~~ dot) corrected using each of the five bias correction techniques for three SSP scenarios for the 2050s (2040-2069) and 2080s (2070-2099). The dark blue circle represents ~~SSP1~~SSP126, light blue represents ~~SSP3~~SSP370 and dark green represents ~~SSP5~~SSP585.

985
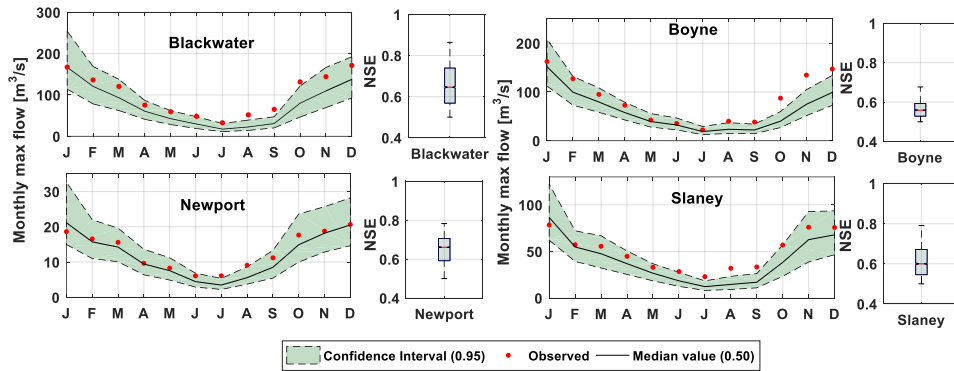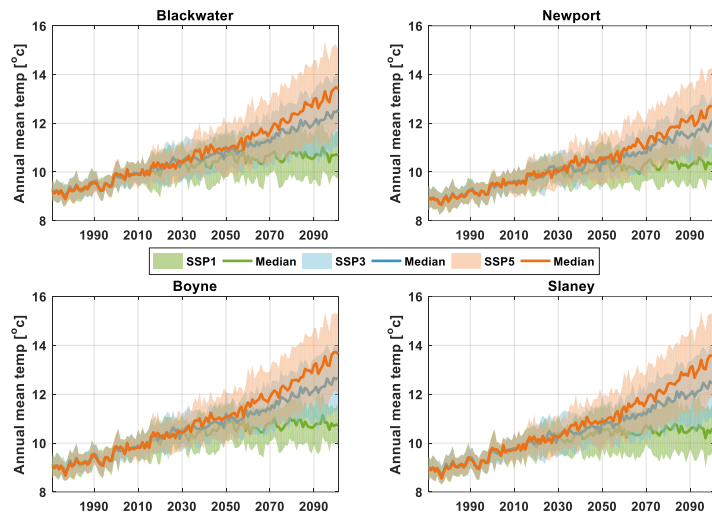
Figure 6. ~~Ensemble of bias corrected simulations of annual mean air temperature (temp) from 12 CMIP6 GCMs for each catchment for the period 1976-2100. Orange, blue and green shaded areas represent the spread of GCM simulations forced using SSP1, SSP3 and SSP5, respectively. The solid lines represent the median of the 12 GCMs for each SSP scenario.~~
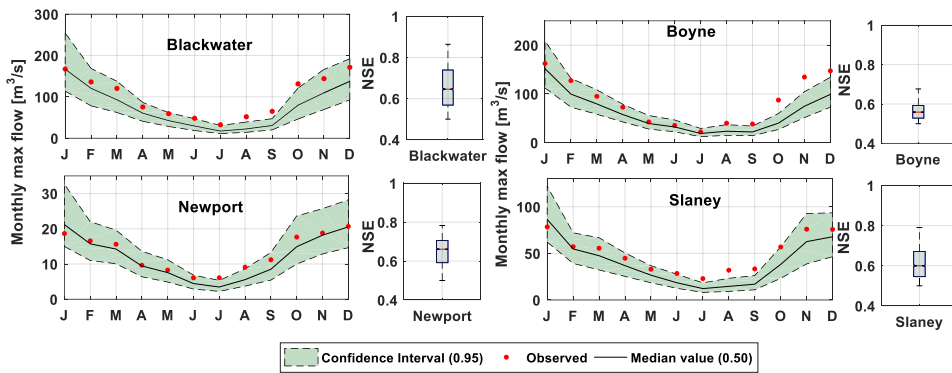
990

Figure 7. Observed and simulated monthly maximum daily flows (m³/s) using GR4J behavioural parameter sets for the reference period (1976-2005). The black line and shaded area represent the median and 95 percent confidence interval of simulated flows, respectively, the red dot represents observed monthly maxima.observations. Boxplots show the spread in NSE scores for behavioural parameters sets in each catchment.

995
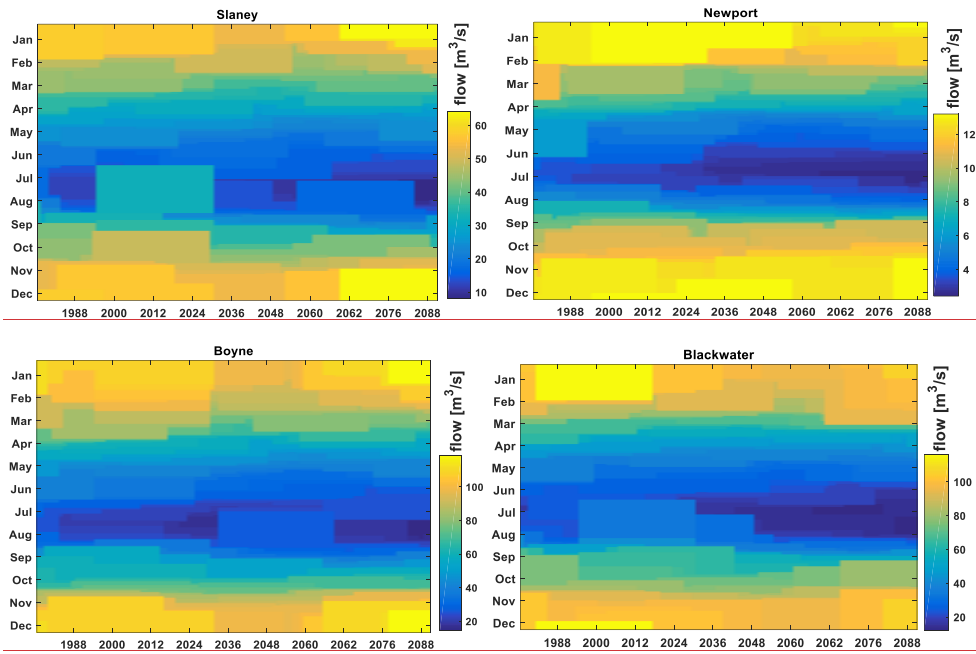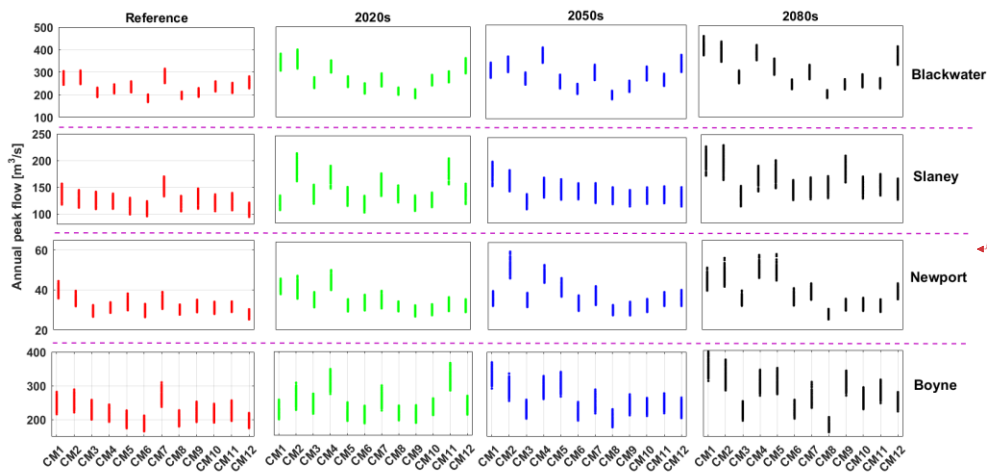
Figure 7. Hydrological model parameter uncertainty in simulating the annual maximum daily~~Figure 8. Ensemble median monthly maximum~~ flow ~~(m³/s) projections for 1976-2100 in~~ in each catchment ~~as simulated~~ using ~~12 CMIP6 GCMs, the five bias correction techniques and~~ the best 300 parameter sets ~~of the hydrological model~~for each climate model for the reference period (red), the 2020s (green), 2050s (blue) and 2080s (black) under SSP370 scenario and DGQM bias correction method.
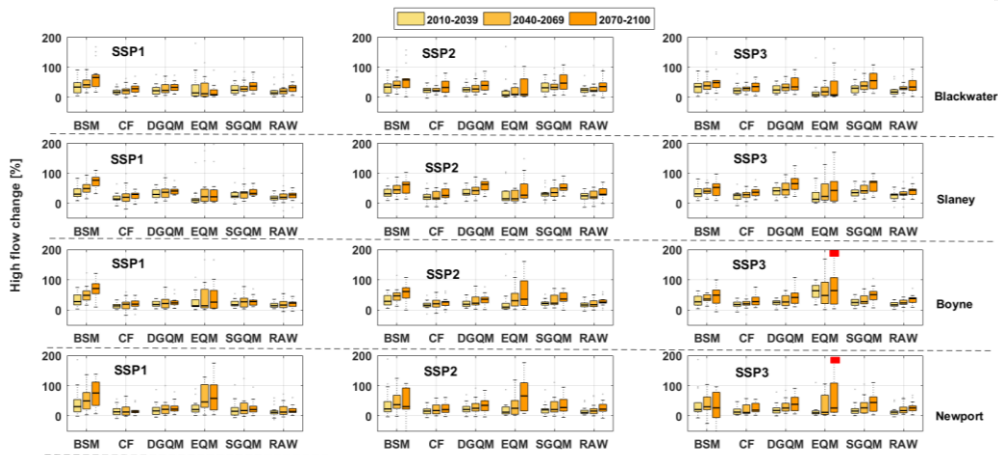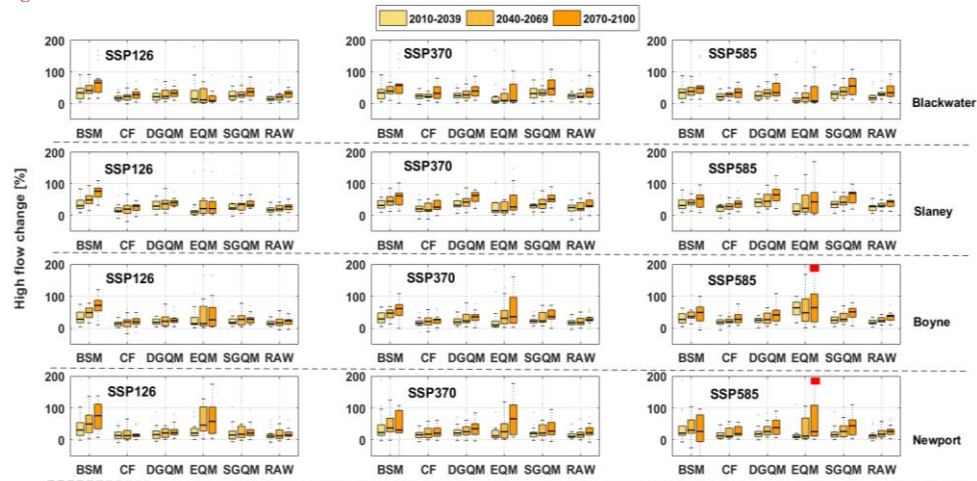
Figure 8. Matrix of projected percent changes in annual maximum ~~river~~daily flow for the 2020s (2010-2039), 2050s (2040-2069), and 2080s (2070-2099) for ~~SSP1, SSP3~~SSP126, SSP370 and ~~SSP5~~SSP585 in each catchment with respect to the reference period (1976-2005). Each box plot represents the spread of 12 GCMs for each of the five bias correction techniques

1015   as simulated using behavioural model parameter sets. Marked for each boxplot are the median and 0.25 and 0.75 quantiles. The red dots are outliers (changes above 200%).
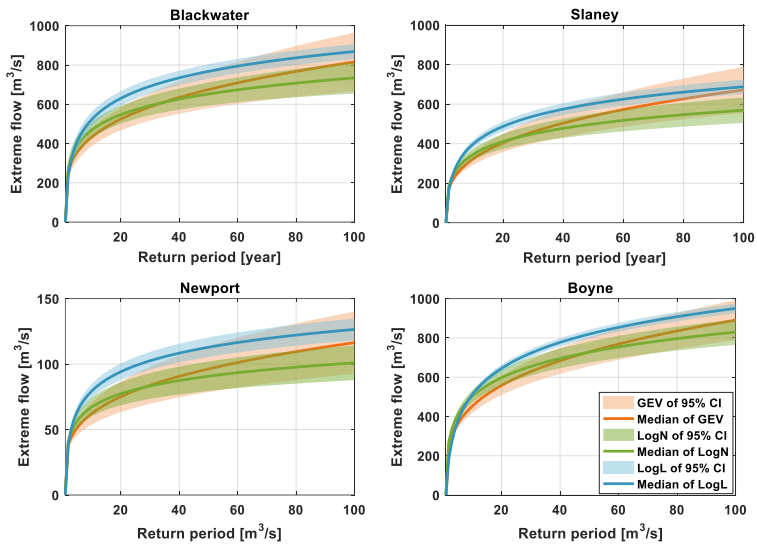
Figure ~~10~~9. Comparison of flood quantiles estimated using three flood distribution models (LogL, GEV and ~~LogN~~LN) fitted to projected annual maxima series ~~using~~ derived from 12 GCMs bias corrected using the DGQM method. The shaded region
1020   indicates the 95% confidence interval of annual maximum projections from 12 GCMs under ~~SSP3~~SSP370 scenario ~~during~~over the full projection period (1970-2100 period) in each catchment.
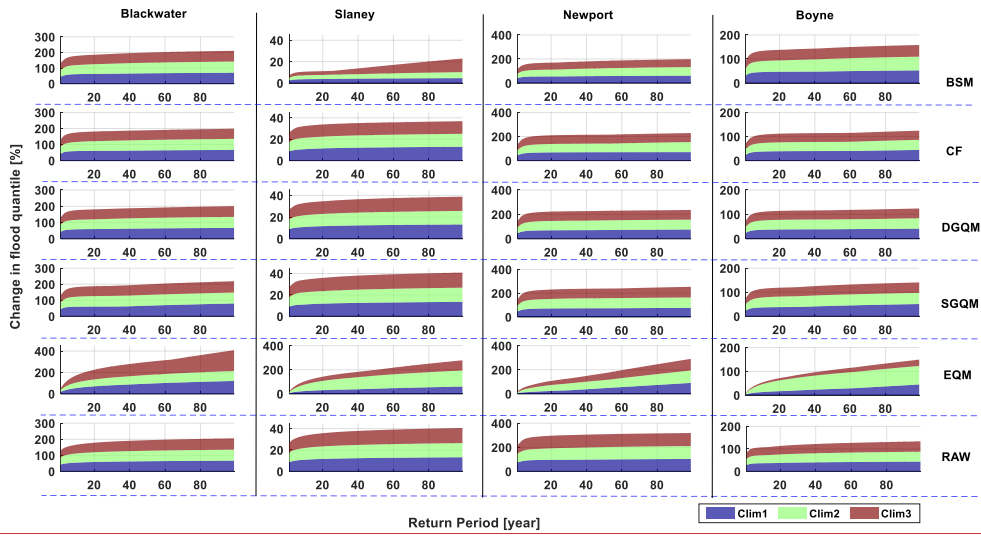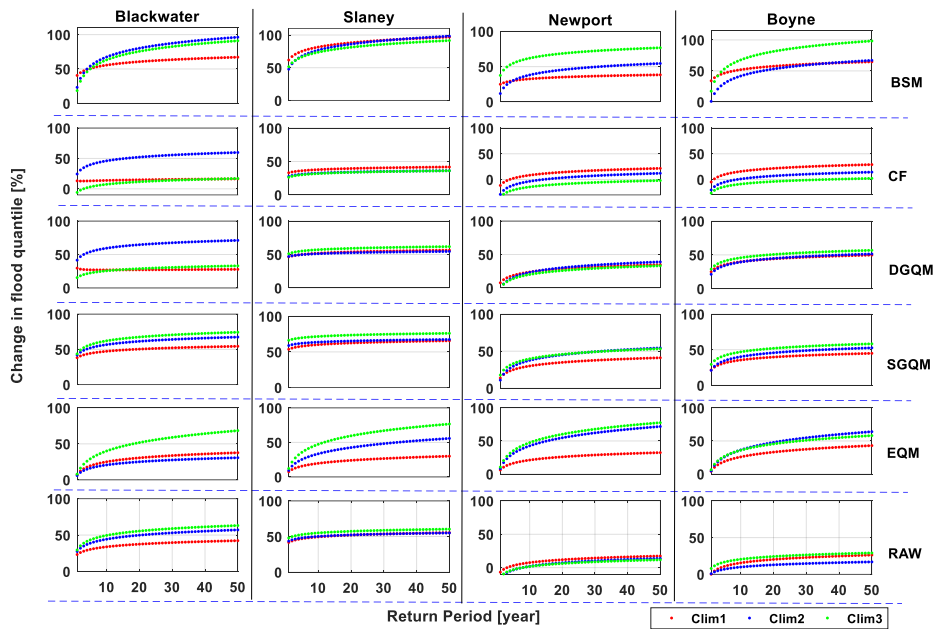
Figure ~~11~~10. Percent changes in extreme flow quantiles using ensemble mean of three distribution types, 12 GCMs and 300 parameter sets in each catchment for the 2020s (~~clim1~~red), 2050s (~~clim2~~blue) and 2080s (~~clim3~~green). Simulated changes are derived using raw (bottom row) and bias corrected (the first four rows) simulations. ~~The shaded region is the spread of 12 climate model and three flood frequency models in the 2020s (blue), 2050s (green) and 2080s (brown) period.~~
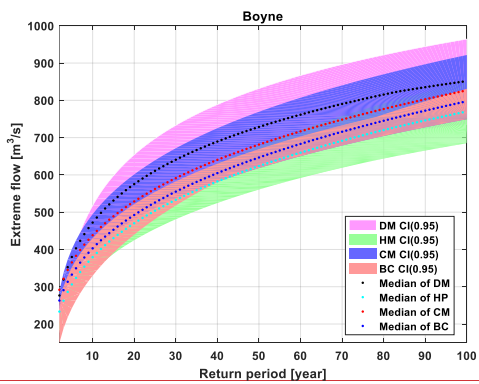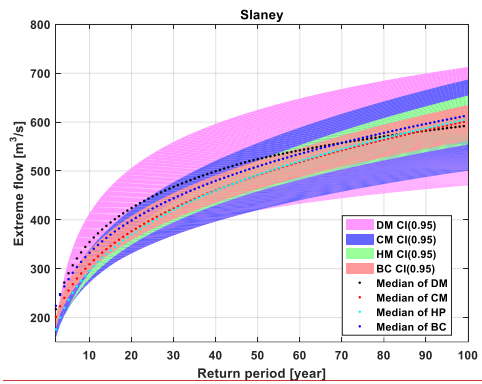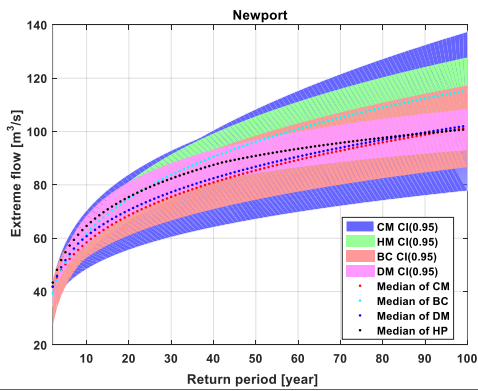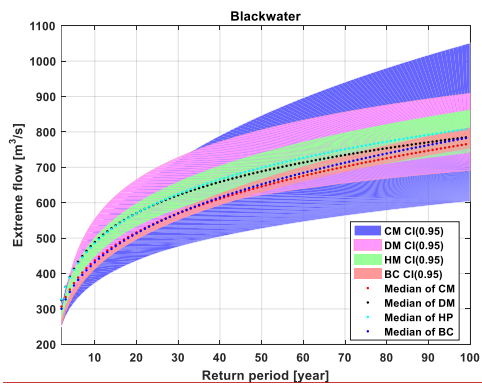
1045

1050

1055
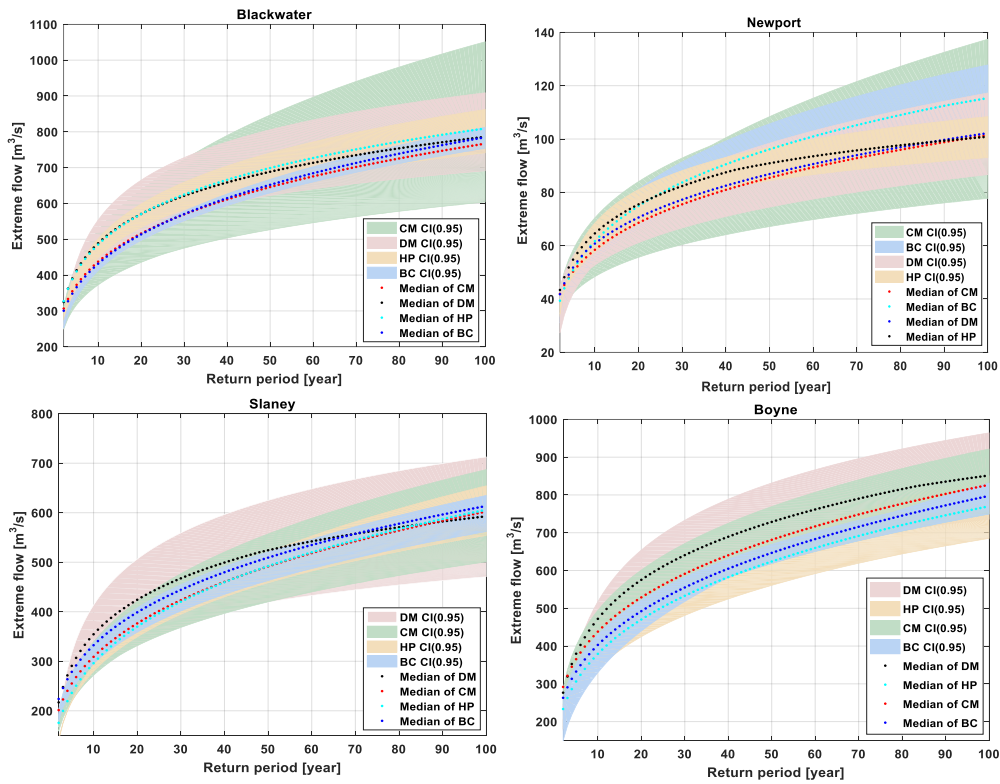
Figure 1211. Total uncertainty in flood frequency curve using 12 CMIP6 GCMs (CM), 5 bias correction methods (BC), 300 behavioural parameter sets (HMHP) and 3 extreme value distributions (DM). Shaded areas represent the 95 percent confidence interval for each component in the modelling chain while the dotted line stands for their respective median values. The curves are fitted to annual maximum time series derived for 1976-2100.
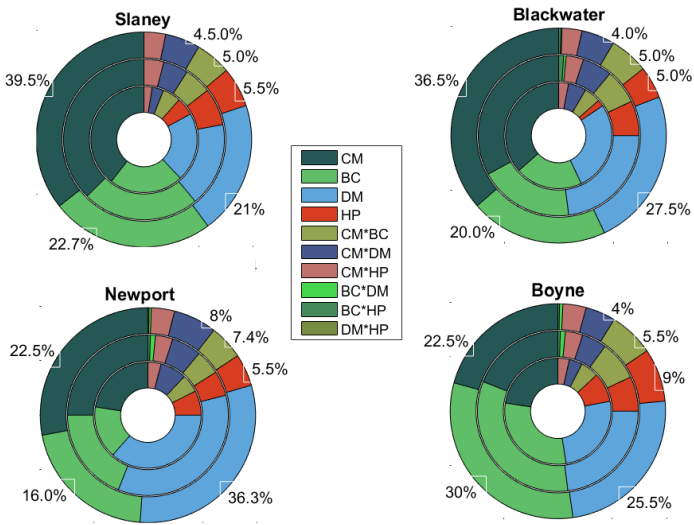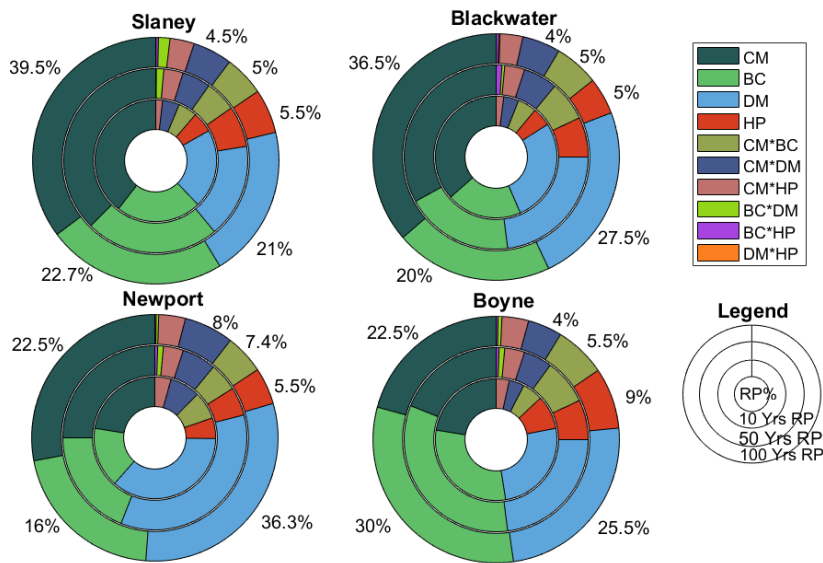
Figure 1312. Contribution of each component of the modelling chain, together with their interaction, to the range of simulated changes in flood riskhazard magnitude for the 2080s (2070-2099) relative to the reference period (1976-2005). Sources considered include 12 CMIP6 climate models (CM), 5 bias correction techniques (BC), hydrological model parameter uncertainty (HP) and 3 extreme value distribution models (DM). The outermost circle/donut represents the flood quantile change at return period (RP) of 100 years, the middle circle RP of 50 years and innermost circle RP of 10 years for the 2080s. Percent changes are annotated for the outermost circle (100-year flood).

Table 1. Statistical and hydro-climatic characteristics of each study catchment.

	Boyne	Blackwater	Slaney	Newport
Latitude [degree]	53.60	52.14	52.~~88~~0	53.95
Longitude [degree]	-6.96	-8.94	-6.61	-9.44
Catchment Area [km²]	2447.36	1257.20	1032.68	146.02
Mean Elevation [m]	70.00	116.00	107.00	56.00
~~95% of river flow value [m³/s]~~	~~95.42~~	~~144.64~~	~~68.76~~	~~14.20~~
~~Annual max flow [m³/s]~~	~~379.09~~	~~351.06~~	~~247.30~~	~~33.40~~
~~95%~~Mean of annual max precipitation ~~value [mm]~~	17.3828.58	24.4639.17	24.0938.23	25.4541.69
Mean ~~Annual~~of annual max ~~precipitation [mm]~~streamflow	45.28232.22	61.76233.59	71.69137.39	93.4824.26
~~Coefficient of Variance of river flow [monthly]~~lower quantile of precipitation (P85)	0.9401	0.7502	0.8201	0.5604
higher quantile of precipitation (P15)	5.46	8.25	6.60	9.95
Low flow (Q95)	4.67	4.47	4.10	0.81
Peak flow (Q5)	106.22	105.40	53.30	16.20
~~Median of annual maximum flow[m³/s]~~Coefficient of Variance of streamflow	214.8337.97	220.6523.79	135.5130.92	24.6018.07
Coefficient of Variance of precipitation ~~[monthly]~~	0.4929.34	0.4724.68	0.5330.86	0.4533.17
Base flow index [-]	0.72472	0.62462	0.73	0.69
Mean of surface runoff [m³/s]	10.21	13.14	5.77	1.86
Mean of base flow [m³/s]	26.85	21.78178	15.58458	4.19

1135

1140

Table 2 List of CMIP6 climate models employed in this study

Code	Institute	Parent source Id	Institution Id
CM1	Commonwealth Scientific and Industrial Research Organisation, Australia	ACCESS-CM2	CSIRO
CM2	Beijing Climate Center, China	BCC-CSM2-MR	BCC
CM3	National Center for Atmospheric Research, USA	CESM2	NCAR
CM4	European: EC-EARTH consortium	EC-Earth	EC-EARTH consortium
CM5	Global Fluid Dynamics Laboratory, USA	GFDL	NOAA-GFDL
CM6	Met Office Hadley Centre, UK	HadGEM3-GC31-LL	MOHC
CM7	JAMSTEC, AORI, NIES, and R-CCS, Japan	MIROC6	MIROC
CM8	Max Planck Institute for Meteorology, Germany	MPI-ESM1-2-HR	MPI-M
CM9	Meteorological Research Institute, Japan	MRI-ESM2-0	MRI
CM10	Nanjing University of Information Science and Technology, China	NESM3	NUIST
CM11	NorESM Climate modeling Consortium, Norway	NorESM2-LM	NCC
CM12	Met Office Hadley Centre, UK	UKESM1-0-LL	MOHC

1145

1150

1155

1160

Supplementary Information

Table S1 Range of hydrological parameters of GR4J model

Parameter	description	L	U
X1	production store capacity [mm]	200	300
X2	Inter-catchment exchange coefficient [mm/d]	0	5
X3	routing store capacity [mm]	10	80
X4	unit hydrograph time constant [d]	0	5

1165

1170
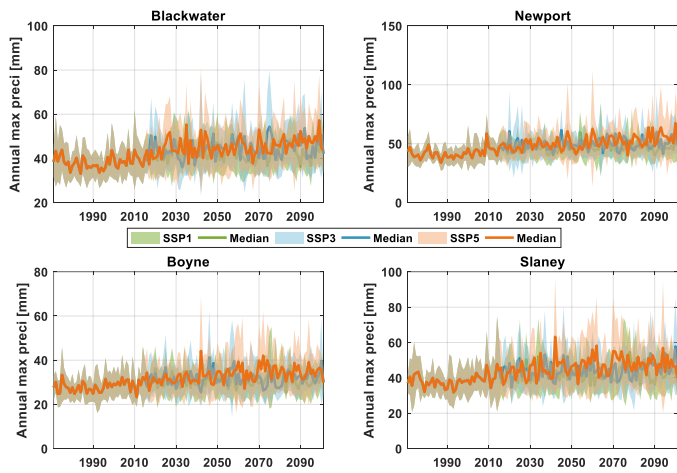
Table S2 in table format of Figure 12

Catchment	RP [yrs]	Main Factors [%]				Interaction of Main factors [%]					
		CM	BC	DM	HP	CM*BC	CM*DM	CM*HP	BC*DM	BC*HP	DM*HP
Blackwater	100	36.5	20	27.5	5	5	4	2	0	0	0
	50	33	19	23	7	7	6	3.5	0.5	1	0
	10	36.33	20.67	23.83	4.83	5.83	5	3	0.17	0.33	0
Boyne	100	22.5	30	25.5	9	5.5	4	3.5	0	0	0
	50	19	33	23	7	8	5	3.5	1	0.5	0
	10	20.75	31.5	24.25	8	6.75	4.5	3.5	0.5	0.25	0
Newport	100	22.5	16	36.3	5.5	7.4	8	4.3	0	0	0
	50	25	19	35	5	5	6	3.5	1	0.5	0
	10	28	20.83	30.67	4.83	5.17	6.5	3.5	0.33	0.17	0
Slaney	100	39.5	22.7	21	5.5	5	4.5	1.8	0	0	0
	50	37.5	23.5	16.5	7.2	5.5	5	3.4	1.3	0.1	0
	10	35.2	23.5	20	5.8	5.3	5.15	3.2	1.5	0.32	0.03
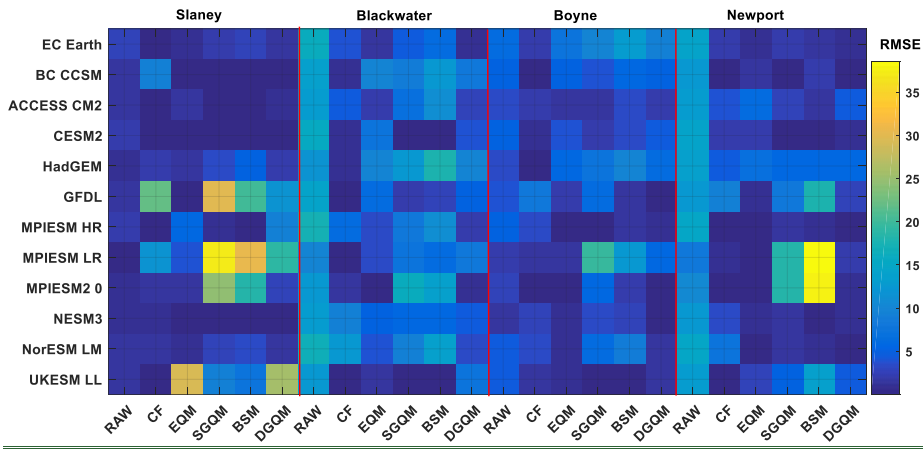
1175

Figure S1. Root Mean Square Error (RMSE) of corrected annual maximum precipitation using five bias correction methods applied to 12 CMIP6 GCMs. The y-axis indicates each climate model and x-axis represents each climate bias correction method.

1180
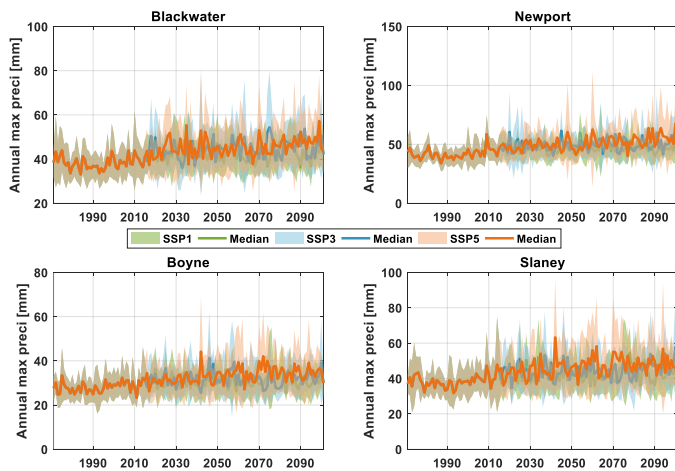
Figure S2. Projected annual maximum daily precipitation as simulated by 12 CMIP6 GCMs forced with SSP1, SSP3SSP126, SSP370 and SSP5SSP585 for each catchment for the period 1976-2100. The orange, blue and green shaded areas represent the model ensemble spread (95% confidence interval) for SSP5, SSP3SSP585, SSP370 and SSP1SSP126, respectively. The solid lines represent the ensemble median for each SSP scenario.

1185

1190
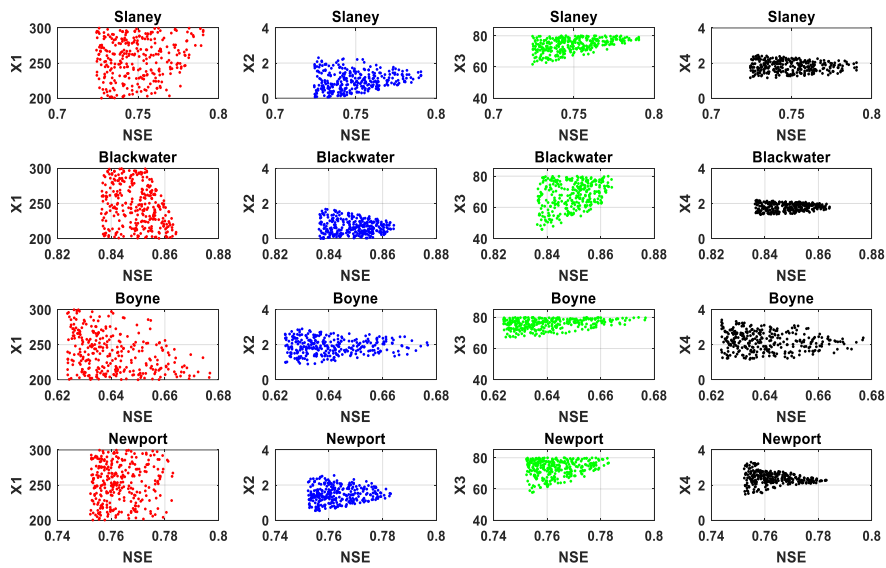
Figure S3. Behavioural parameter sets for the GR4J model for each catchment and their respective NSE objective function distribution. The red (X1 parameter), blue (X2 parameter), green (X3 parameter) and black (X4 parameter) dots represent the best values of the NSE objective function for respective GR4J model parameter values.

1195

Formatted: Font: Not Bold
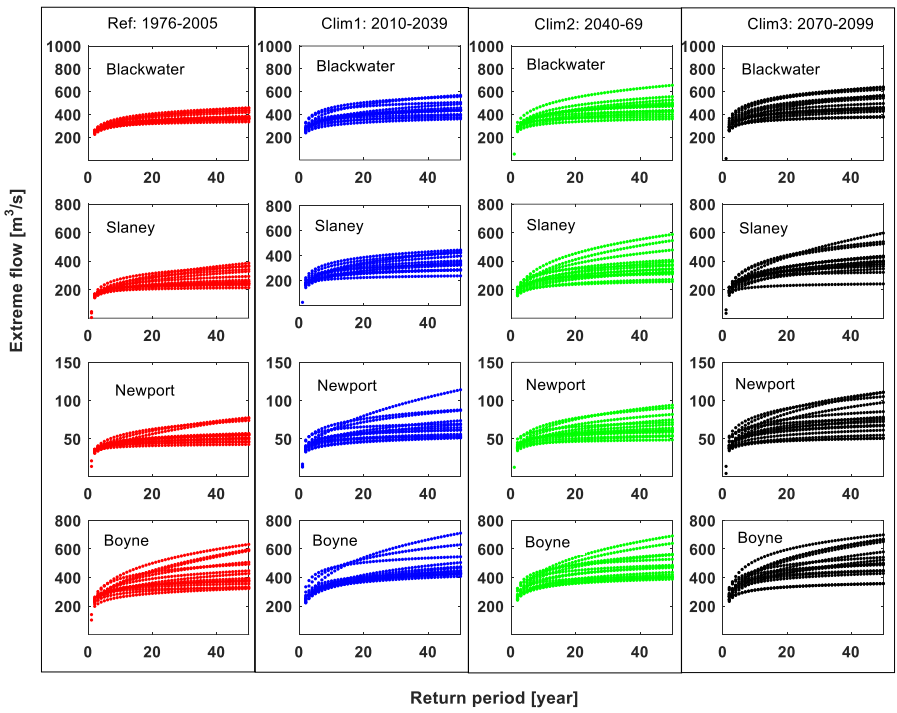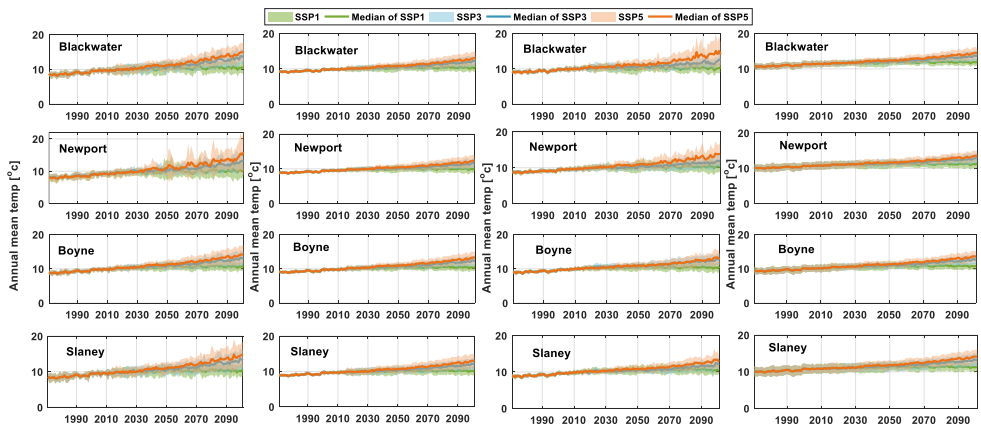
Figure S3. Comparison of temperature bias correction using BSM (first column from left), CF (second column from left), EQM (third column from left) and the fourth column is uncorrected air temperature for each catchment.

Formatted: Font: Not Bold
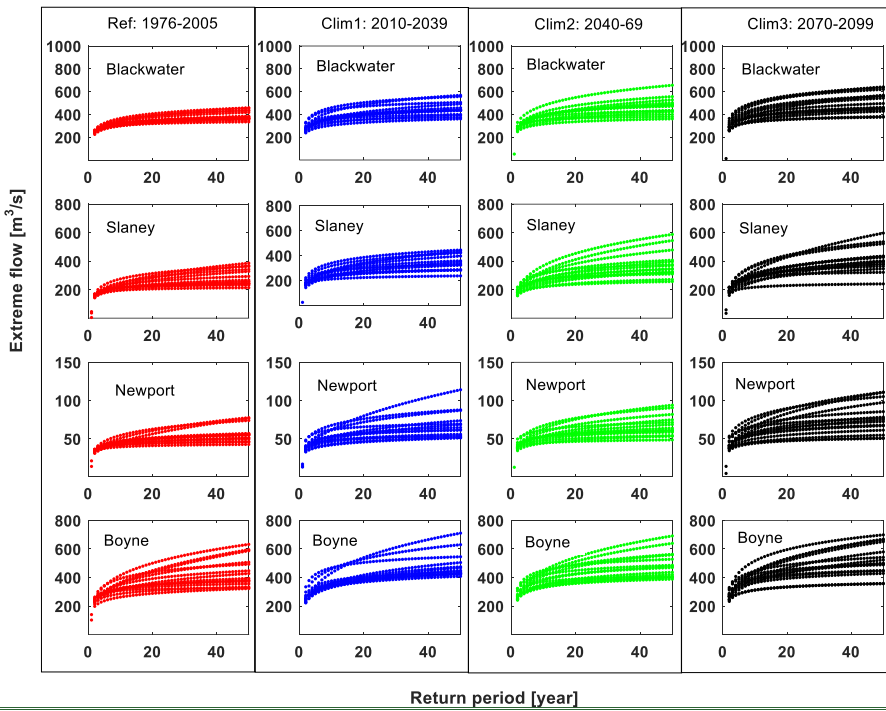
Figure S4. Flood frequency curves using GEV distribution model at different return periods for the reference period (1976-2005), the 2020s (2010-2039), the 2050s (2040-2069) and the 2080s (2070-2099) in each of the four study catchments. Each colour represents each climate period, red for reference period, blue very near future, green near future and black far future. Each line in each colour represent single climate model simulated from the best hydrological parameter set and DGQM bias correction.

Figure S1. Root Mean Square Error (RMSE) of corrected annual maximum precipitation using five bias correction methods applied to 12 CMIP6 GCMs. The y-axis indicates each climate model and x-axis represents each climate bias correction method.

1230